Co-firing Coal: Feedlot and Litter Biomass Fuels

Quarterly Progress Report # 8

Grant #: **DE-FG26-00NT40810**

Project Name: *Feedlot and Litter Biomass Co-firing in Pulverized Fuel and Fixed Bed Burners*

Contractor name: Texas Engineering Experiment Station, Texas A&M University

Sponsor: US Dept of Energy, National Energy Technology Laboratory

Principal Investigator: Dr. Kalyan Annamalai, Mech. Eng., Texas A&M, College Station, TX 77843-3123
979-845-2562
Kannamalai@mengr.tamu.edu

Other Investigators: Dr. John Sweeten, Professor of Agricultural Eng. and Resident Director of Agricultural Extension Service,
Dr. Saqib Mukhtar, Asst. Prof., Agricultural Engineering.

Graduate Students: Ben Thien (PhD)
Gengsheng Wei (PhD)
Soyuz Priyadarsan (MS)

Quarterly Report #: 8

Report Period: 3/15/02-6/14/2002

PROGRESS REPORT # 7

A. Proposed activities for quarter 8 (3/15/2001 – 6/14/2002)

Boiler Burner Simulation and Experiments:

1. Continue the parametric study of cofiring of pulverized coal and LB in the boiler burner, and determining the combustor performance and emissions of NO, CO, CO_2, PO_2 and P_4O_{10}, etc. The air-fuel ratio, swirl number of the secondary air stream and moisture effects will also be investigated (Task 4).

Gasification: (Task 3)

2. Measuring the temperature profile for chicken litter biomass under different operating conditions.
3. Product gas species for different operating conditions for different fuels.
4. Determining the bed ash composition for different fuels.
5. Determining the gasification efficiency for different operating conditions.

B. Achieved during quarter 8 (3/15/2001 – 6/14/2002)

Boiler Burner Simulation and Experiments:

1. The evaporation and phosphorus combustion models have been incorporated into the PCGC-2 code. Mr. Wei has successfully defended his Ph.D. proposal on Coal: LB modeling studies (Task 4, Appendix C).
2. Reburn experiments with both low and high phosphorus feedlot biomass has been performed (Task 2, Appendix A).
3. Parametric studies on the effect of air-fuel ratio, swirl number of the secondary air stream and moisture effects have been investigated (Task 2, Appendix A).
4. Three abstracts have been submitted to the *American Society of Agricultural Engineers Annual International* meeting at Chicago in July 2002. Three part paper dealing with fuel properties, cofiring, large scale testing are still under review in the *Journal of Fuel*.

Gasification: (Task 3, Appendix B)

5. Items # 2, and 3 are 95 % complete, with four more experiments yet to be performed with coal and chicken litter biomass blends.
6. Item # 4, and 5 shall be performed after completion of all the experiments.

C. Proposed activities for quarter 9 (6/15/2001 – 9/14/2002)

Fuel Properties: (Task 1b)

1. Submit a full paper on fuel properties to the American Society of Agricultural Engineers.

Gasification: (Task 3)

2. Complete experiments with coal and chicken litter biomass blends.
3. Determine bed ash composition for different fuels.
4. Determine the gasification efficiency for different operating conditions.

Modeling and Simulation: (Task 4)

5. Complete the modeling task (which will lead to the defense of Mr. Wei's Ph.D. thesis)

Milestone Log- **DE-FG26-00NT40810-Annamalai-**Quarter # 8; **Report Period**: 3/15/02-6/14/2002.

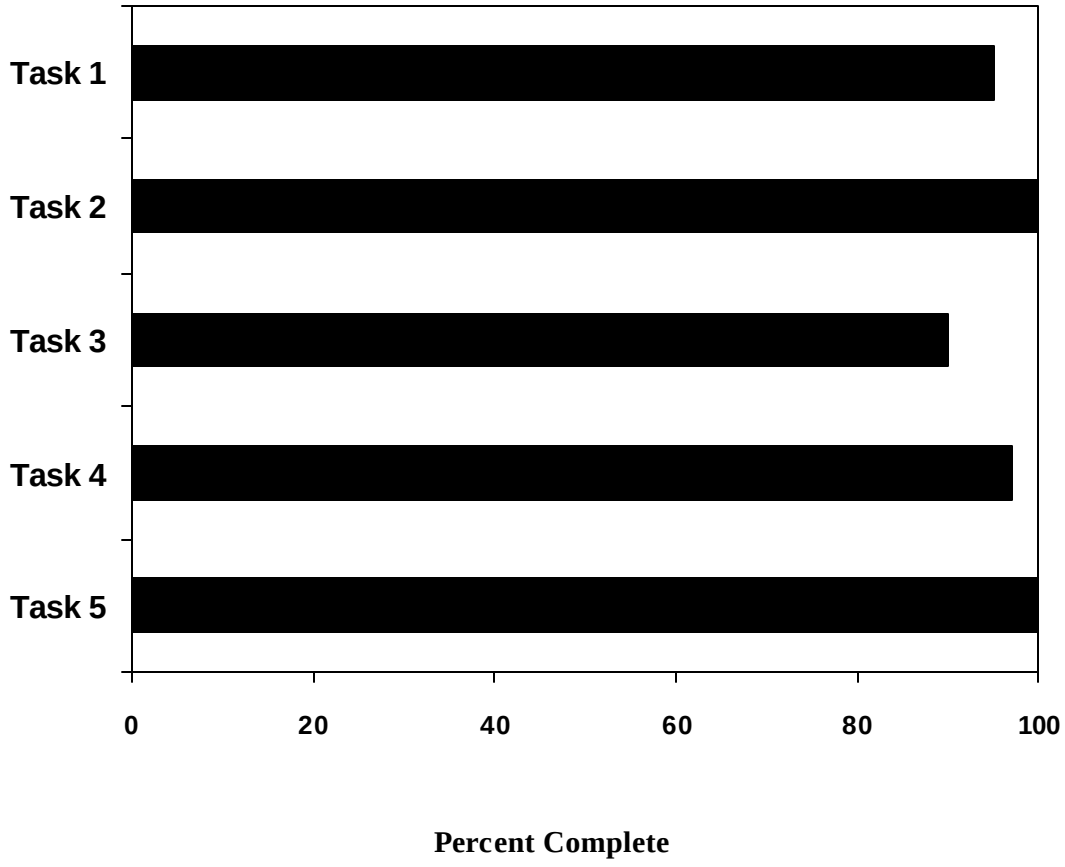

Appendix A: Boiler Burner Experiments (Task 2)

A) Cofiring of CLB fuels:

1a.1. Size effects

The effect of different biomass particle sizes was investigated by size classifying the litter biomass into 3 size groups: a 0-75 μm size group, a 75-150 μm size group, and a 150+ μm size group. Biomass can be harder to grind than coal, and experience a larger variation of size. The effect of different sizes must be investigated before larger scale co-firing can be attempted. The fuels were fired at 10% excess air using the same experimental parameters. Figure 2a.1 shows the effect of the difference particle sizes on the CO emissions. The CO emissions are the same for all of the size classes except for the largest size class. The larger particles take longer to burn, resulting in less complete combustion and a higher CO emissions level. The effect of biomass particle size on O_2 emissions is show in figure 2a.2. The different size groups do not appear to have different O_2 emissions levels, but the full size group appears to have a slightly higher O_2 level due to variations in the experiments. The burnt mass fraction is shown in figure 2a.3 for the different size groups. The level of combustion seems to be fairly constant for all of the size groups, expect for the full size group, because of its lower oxygen concentration. Now the NO emissions are seen on a uncorrected ppm basis in figure 2a.4. The results again show similar level across all of the different size groups. Finally, the NO emissions are show in figure 2a.5 on a kg/GJ basis. Again, it is seen that there are no large differences between the different size groups.

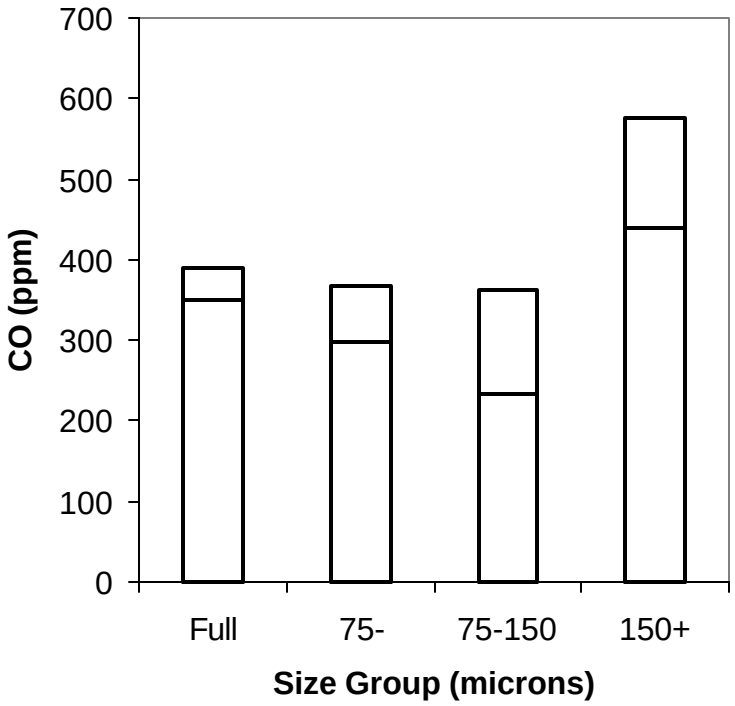

Figure 2a.1: Effect of biomass particle size on CO emissions

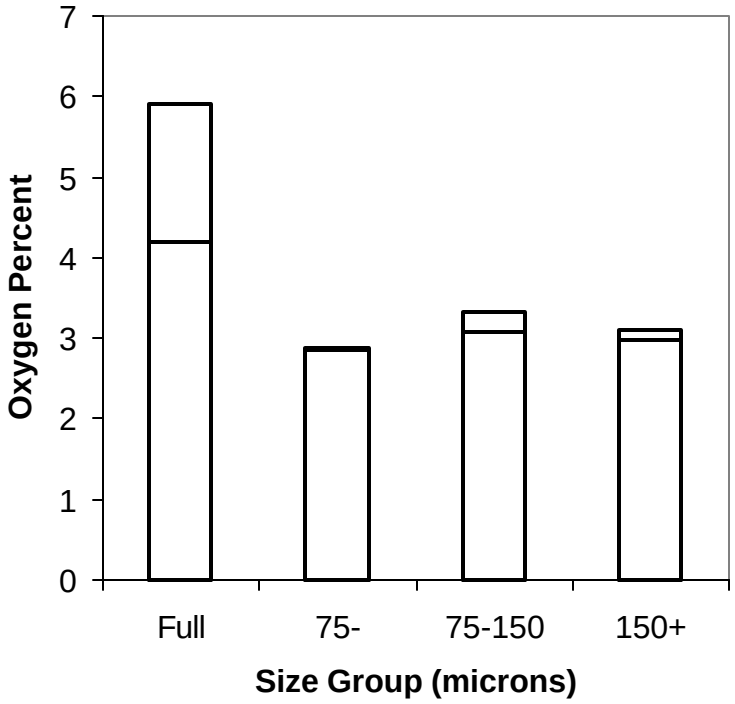

Figure 2a.2: Effect of biomass particle size on O_2 emissions

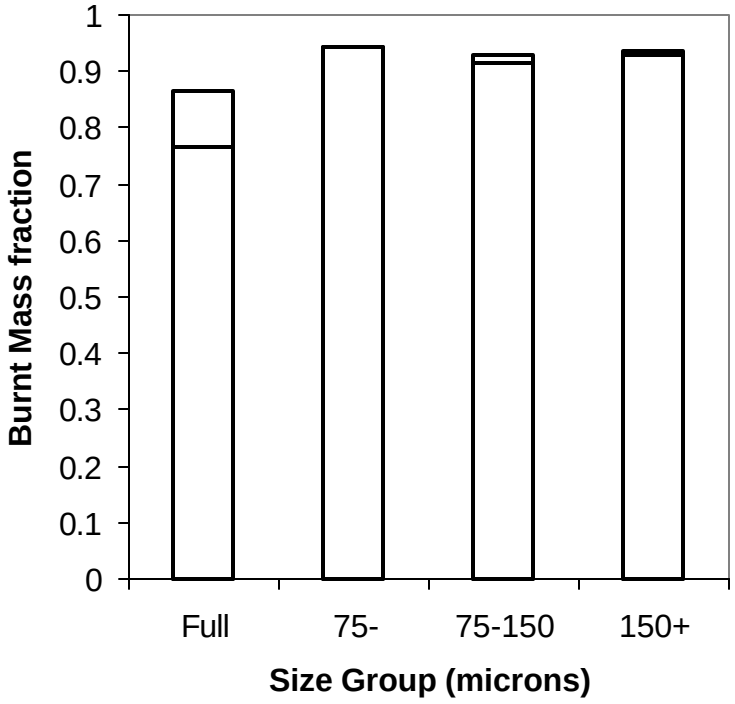

Figure 2a.3: Effect of biomass particle size on burnt mass fraction

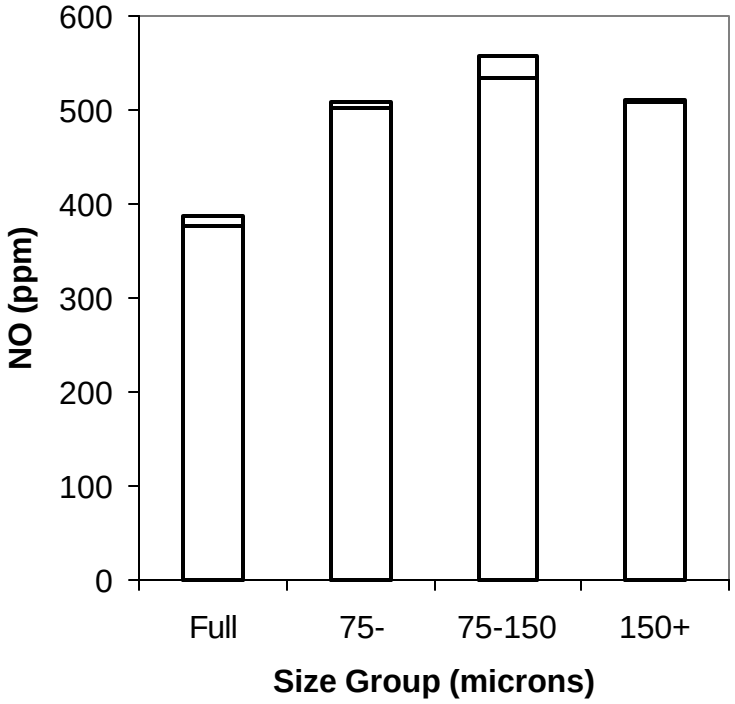

Figure 2a.4: Effect of biomass particle size on NO emissions (uncorrected)

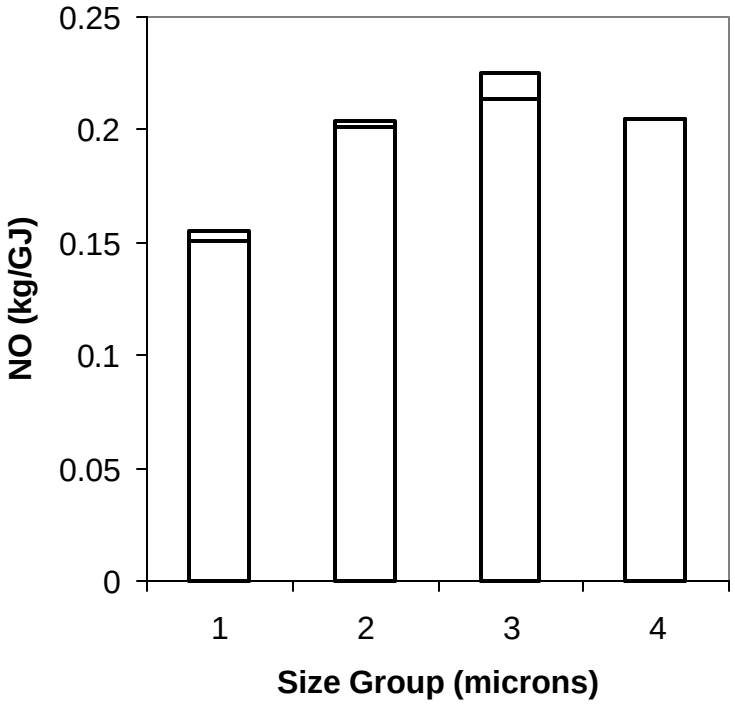

Figure 2a.5: Effect of biomass particle size on NO emissions on a heat basis

1a.2. Swirl Effects

The effect of changing the swirl number was also investigated. The swirl at the top of the furnace was removed and replaced with a swirler with a fin angle of 55° to get a secondary air swirl number of 1. The original swirl burner had a secondary air swirl number of 0.7 and a swirl angle or 45°. The effect of the altered swirl number on CO emissions is shown in figure 2a.6. There is little change between the high swirl and the low swirl burner. The effect of changing swirl on the O_2 emissions is shown in figure 2a.7. The higher swirl results in a lower oxygen concentration. The high swirl number results in greater turbulence, and a faster mixing of fuel and air, which lowers the oxygen concentration. The effect of swirl number on the burnt mass fraction is shown in figure 2a.8. The result of greater mixing in again seen in the burnt mass fraction, where the greater mixing results in a greater burnt mass fraction. The swirl also influences the NO emissions, seen on a ppm basis in figure 2a.9, and on a kg/GJ basis in figure 2a.10. The greater swirl and mixing translates to higher levels of NO emissions. The fuels are mixed faster, bringing the fuel N and Oxygen together sooner, and allowing more time for NO formation.

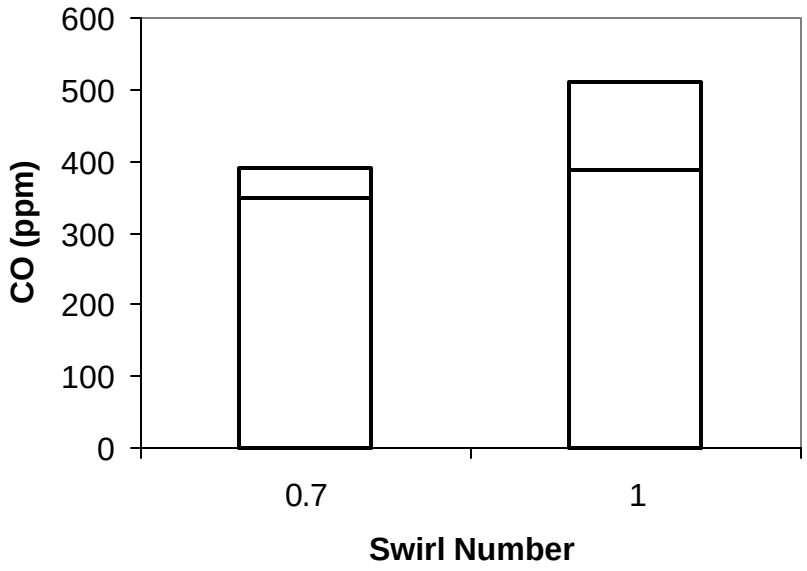

Figure 2a.6: Effect of swirl number on CO emissions

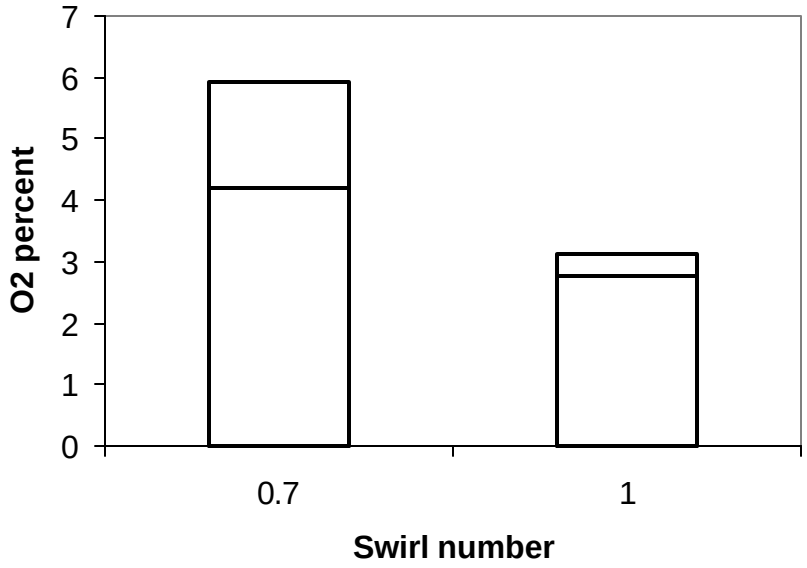

Figure 2a.7: Effect of Swirl number on O_2 emissions

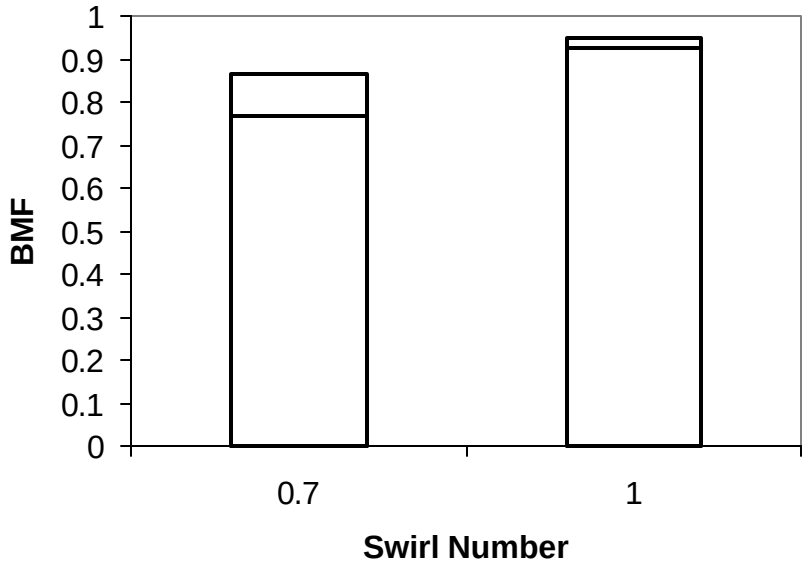

Figure 2a.8: Effect of Swirl number on BMF

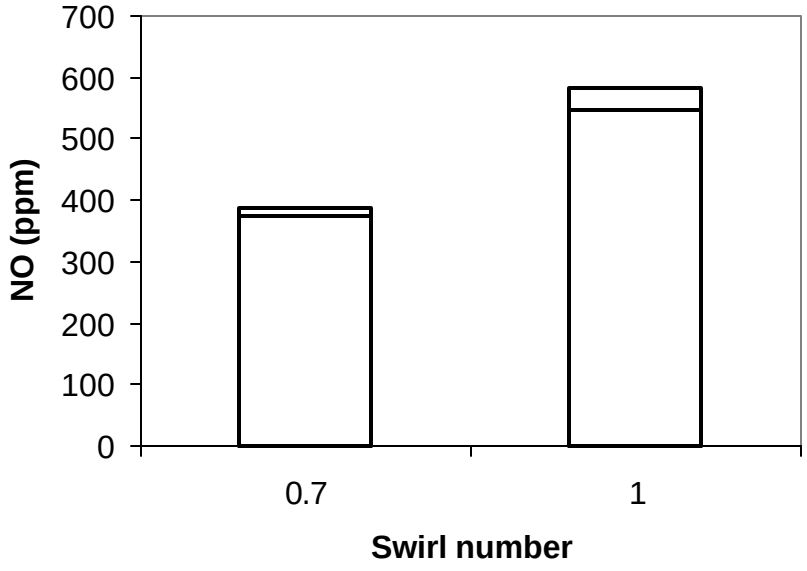

Figure 2a.9: Effect of swirl number on NO

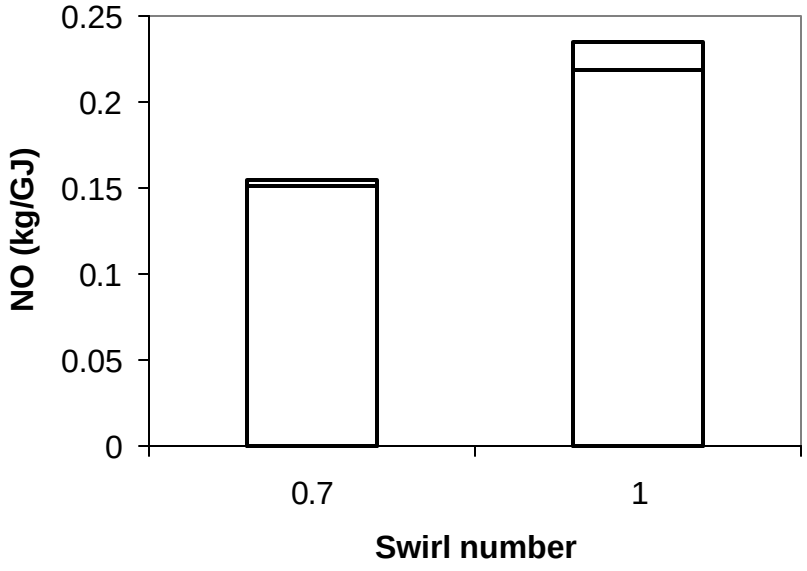

Figure 2a.10: Effect of swirl number on NO emission (heat basis)

1a.3. Biomass moisture effects

Next, the effects of different manure moisture contents were investigated. The biomass used in these experiments was dried to allow for grinding and easier handling. In an industrial setting, drying may not be possible, and it is necessary to investigate the effect that a high level of biomass moisture will have on the combustion parameters. For these experiments, water was mixed with the coal and the biomass to simulate biomass moisture with 30% dry loss. The resulting CO emissions are given in figure 2a.11. The results show that the higher biomass

moisture will translate into high CO emissions by creating more CO through reaction between steam and the fuel char. The O_2 emissions for high and low biomass moisture levels are given in figure 2a.12, and the burnt mass fraction are shown in figure 2a.13. The burnt mass fractions appear similar in both cases. The reduction in heating value caused by the addition of water is made up by faster reaction with steam, which allows the fuels to achieve similar level of burnt mass fraction. Finally, the NO emissions are shown on a ppm basis in figure 2a.14, and on a heat basis in figure 2a.15. Lower levels of NO emission were obtained with the low moisture fuel. The higher water content will result in lower flame temperatures, and a corresponding drop in the formation of NO from atmospheric nitrogen.

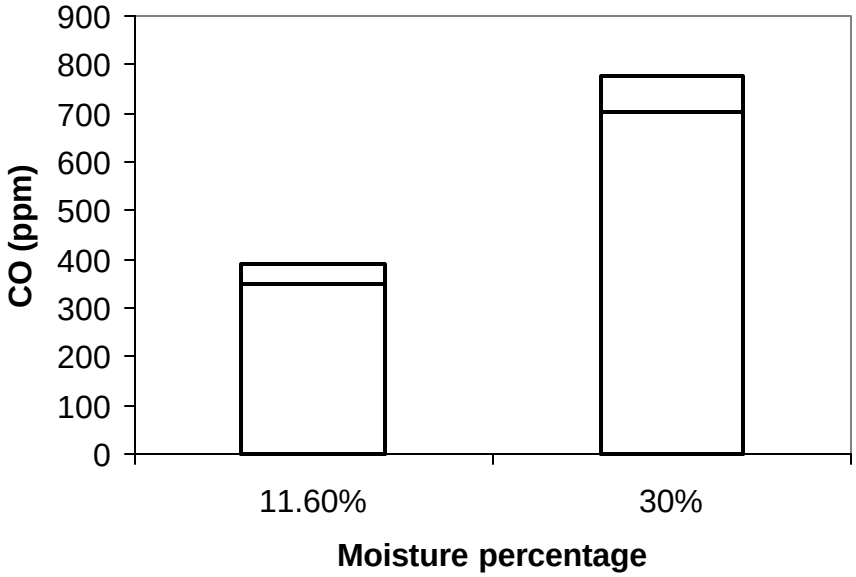

Figure 2a.11: Effect of biomass moisture percentage on CO emissions

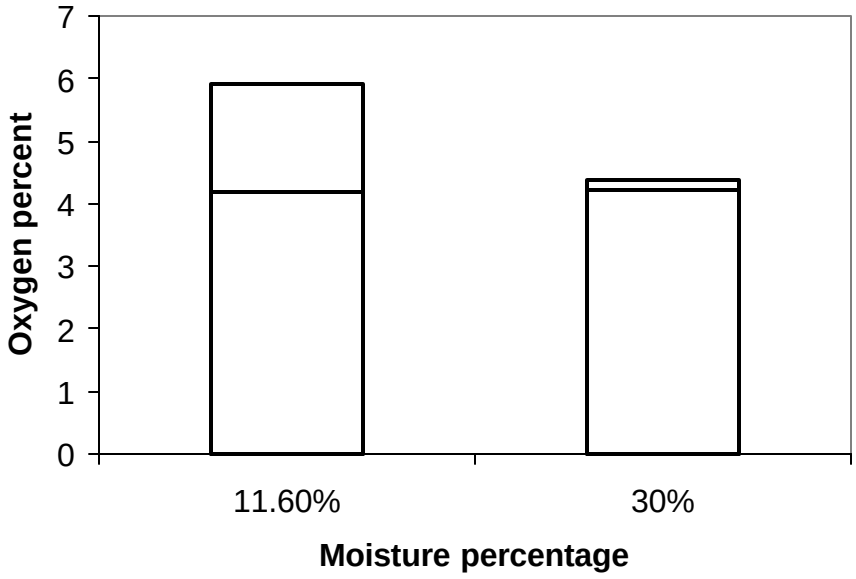

Figure 2a.12: Effect of biomass moisture percentage on O_2 emissions

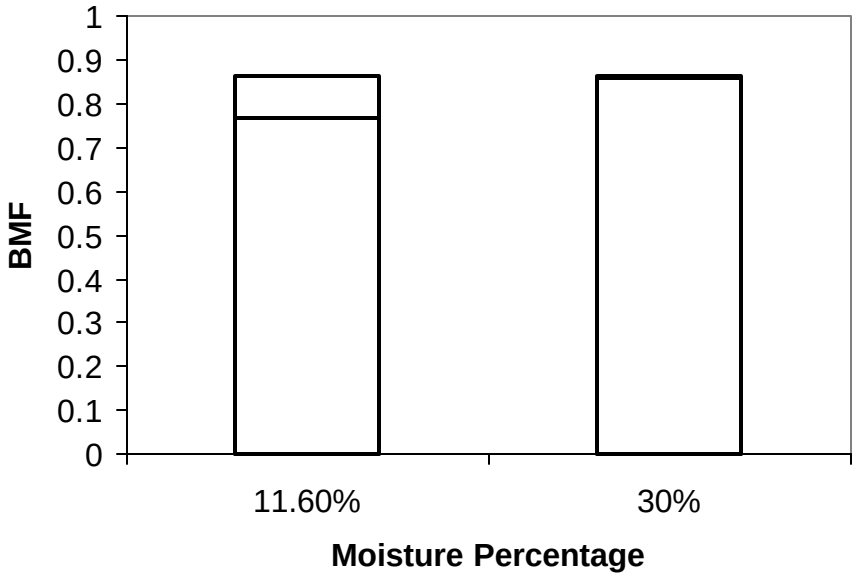

Figure 2a.13: Effect of biomass moisture percentage on burnt mass fraction

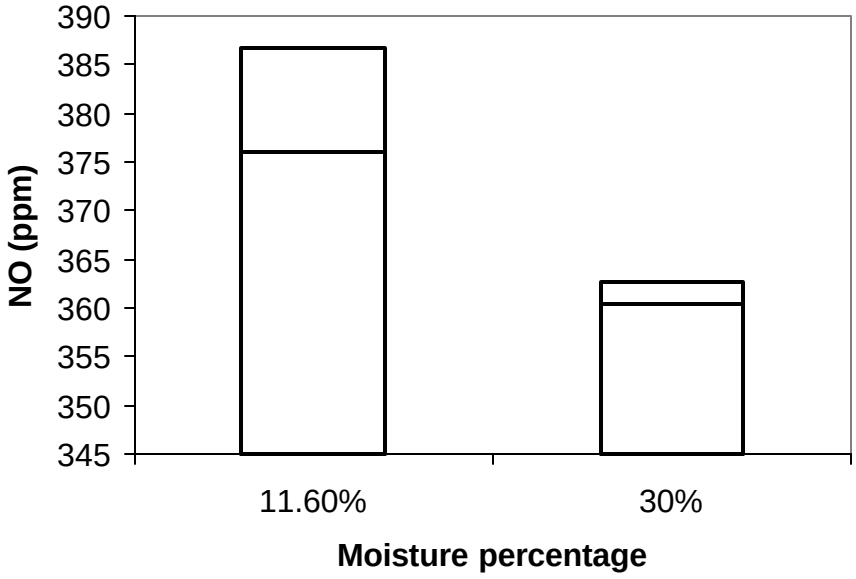

Figure 2a.14: Effect of biomass moisture percentage on NO emissions

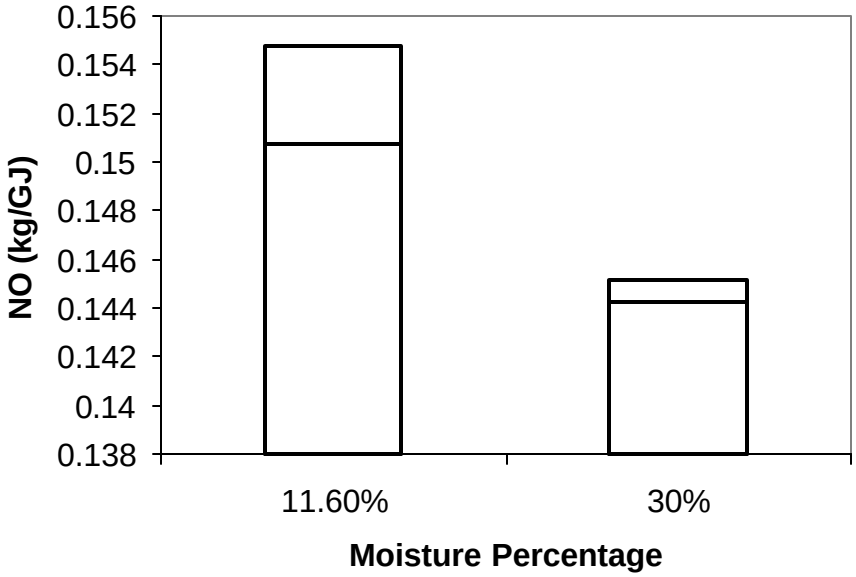

Figure 2a.15: Effect of biomass moisture percentage on NO emissions (heat basis)

1a.4. Loading ratio

The effect of different loading ratios on the combustion performance was also investigated. The loading ratio is the mass of fuel in the primary air stream divided by the mass of air in the primary air stream. When a higher loading ratio was tried, with more fuel in the stream, the greater fuel density caused clogging in the venturi, and uneven combustion results

were obtained. The variation of CO with loading ratio is shown in figure 2a.16, and the variation of O_2 with loading ration is shown in figure 2a.17. The clogging of the fuel feeder created burst of fuel, which resulted in the high CO and lower O_2 levels as burst of fuel would cause spikes of high CO and low oxygen. The effect of the primary air-loading ratio on the burnt mass fraction is shown in figure 2a.18. Finally, the NO emissions on a ppm basis and on a heat basis are shown in figures 2a.19 and 2a.20. The higher loading ration resulted in a higher NO emissions, but the results are unreliable due to the problems with feeding the fuel at the higher loading ratio.

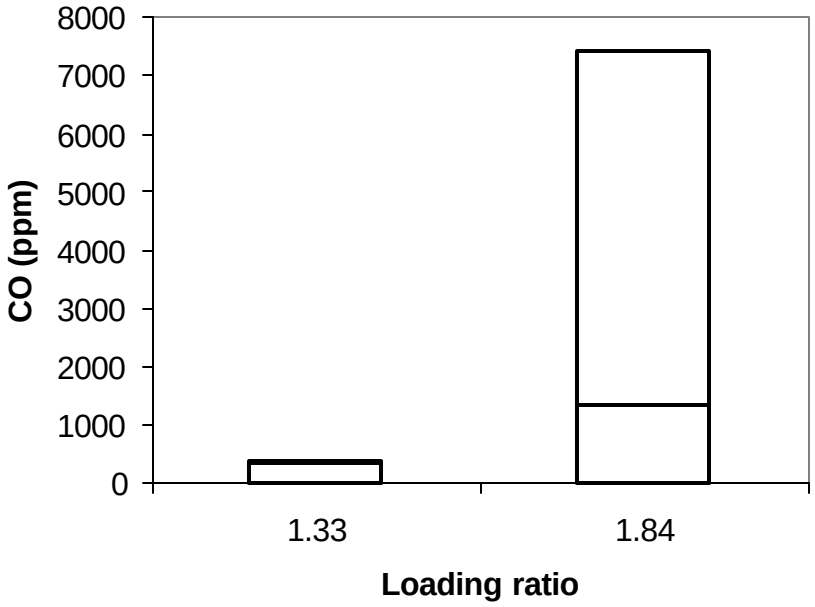

Figure 2a.16: Effect of primary air loading ratio on CO emissions

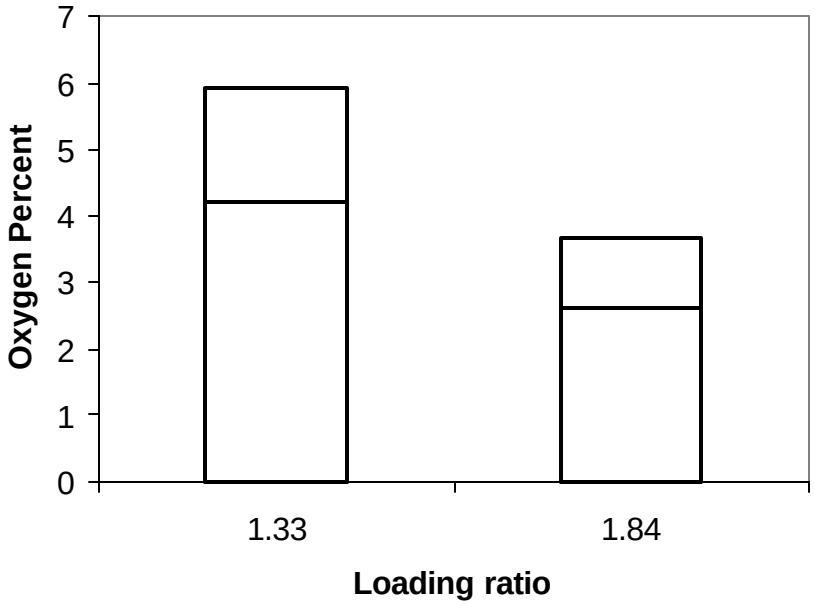

Figure 2a.17: Effect of primary air loading ratio on O_2 emissions

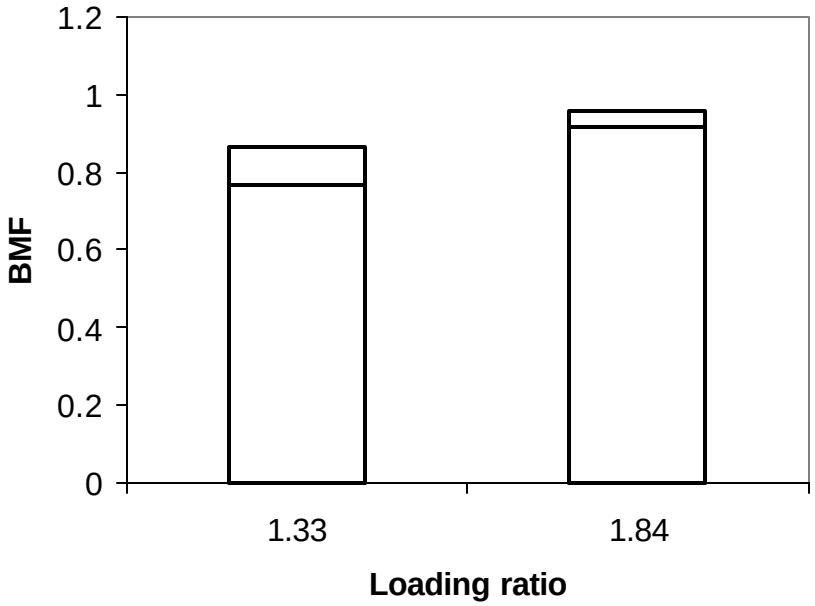

Figure 2a.18: Effect of primary air loading ratio on burnt mass fraction

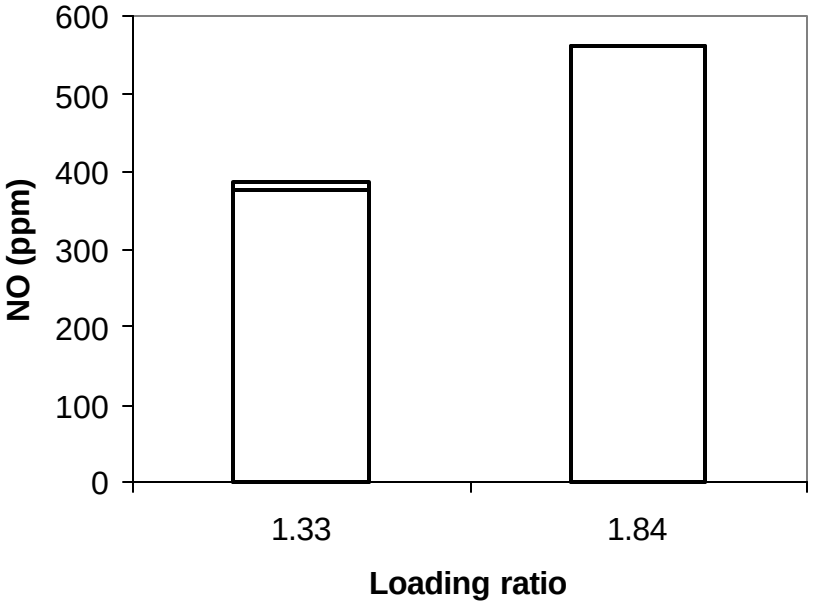

Figure 2a.19: Effect of primary air loading ratio on NO emissions

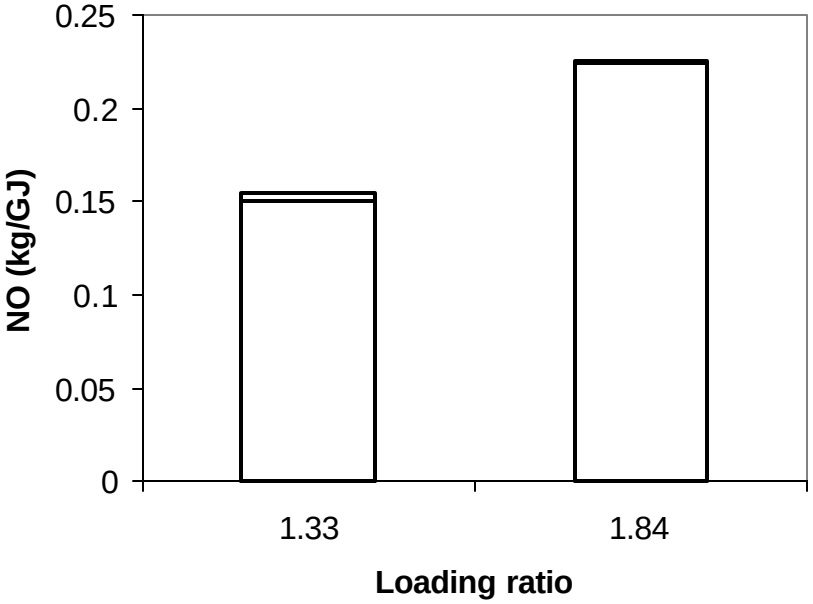

Figure 2a.20: Effect of primary air loading ratio on NO emissions (heat basis)

B) Reburning of CFB fuels:

For this project, a cattle-feeding trial was conducted to produce two different types of manure for combustion studies. Manure for this project was removed from TAES/ARS Environmental feedyard at Bushland, Texas. The two types of manure produced were Low ash and low phosphorus manure and low ash standard (high) phosphorus manure. This manure was partially composted and dried down in the greenhouses at TAES/ARS research laboratory at Bushland. The combustion characteristics of this manure will be tested at Texas A&M University. This study is the thesis work of Kevin Heflin at West Texas A&M University and will be presented at the annual international American Society of Agricultural Engineers conference in Chicago, July 2002.

The results in the following tables will be expanded upon in the next quarterly report. At this time, only the raw data is available.

TAES Bushland Environmental Feedyard Manure Project VII
Cattle manure that is currently being composted from fly ash surfaced pens 10-15
Temperature F

	Date	**11/9/01**	**11/30/01**	**12/7/01**	**12/10/01**
LP Compost	Grand mean +/- std.dev.	102.67+/- 1.15	119.43+/- 11.86	109.69+/- 8.45	105.67+/- 7.87
HP Compost	Grand mean +/- std.dev.	90.67+/- 8.08	127.57+/- 14.77	120.00+/- 8.02	123.33+/- 6.38

TAES Bushland Environmental Feedyard Manure Project VII
Cattle manure that is currently being composted from fly ash surfaced pens 10-15
% Moisture w.b.

		11/9/01	**12/3/01**	**12/7/01**	**12/10/01**
LP Compost	Grand mean +/- std.dev.	12.55 +/-098	40.19+/-6.98	30.69+/-2.98	45.69+/-0.77
HP Compost	Grand mean +/- std.dev.	15.28 +/-4.19	24.82+/-1.56	31.64+/-2.38	49.48+/-0.90

TAES Bushland Environmental Feedyard Manure Project VII
Cattle manure that is currently being composted from fly ash surfaced pens 10-15
% Ash

	Manure from	**11/9/01**	**12/10/01**
Pens 10,13,14	Fly ash surface Low phosphorus Grand mean +/- std.dev.	14.49+/- 0.74	17.68+/- 1.04
Pens 11,12,15	Fly ash surface High phosphorus Grand mean +/- std.dev.	17.86+/- 2.51	19.91+/- 1.31

Gas characteristics as measured by an ENERAC 3000 gas analyzer during co-fire testing at Texas A&M

Results from A&M Co-fire project 7 **May 14-17, 2002**
Gas Analyzer results

Low phosphorus manure blended 90/10

Date	Time	Combust Efficiency	Ambient Temp	Stack Temp	O2 %	CO ppm	CO2 %	Combustibles	Excess air	Nitric oxide	Nitrogen dioxide	NOX	SOX
5/14/02	10:52	54.60	79.00	502.00	3.10	1202.00	14.30	3.21	12.00	347.00	3.00	350.00	19.00
5/14/02	10:53	52.80	80.00	553.00	3.00	1218.00	13.90	3.50	12.00	344.00	3.00	347.00	22.00
5/14/02	10:54	51.30	80.00	601.00	3.20	1040.00	13.80	3.21	13.00	356.00	3.00	359.00	22.00
5/14/02	10:55	41.10	80.00	615.00	3.00	1130.00	13.70	3.78	12.00	351.00	3.00	355.00	23.00
5/14/02	10:56	49.30	80.00	632.00	3.20	1119.00	13.20	3.21	14.00	360.00	3.00	363.00	24.00
5/14/02	10:57	38.30	80.00	642.00	3.20	1045.00	13.00	4.07	14.00	364.00	3.00	367.00	24.00
5/14/02	10:58	37.90	80.00	647.00	3.00	1474.00	12.90	4.36	13.00	359.00	0.00	359.00	24.00
5/14/02	10:59	37.30	80.00	656.00	3.10	1186.00	12.80	4.36	14.00	362.00	0.00	362.00	39.00
5/14/02	11:00	36.60	80.00	662.00	3.00	13.05	12.60	4.36	13.00	355.00	0.00	355.00	40.00
5/14/02	11:01	36.60	80.00	668.00	3.10	1156.00	12.60	4.36	14.00	361.00	0.00	361.00	48.00
5/14/02	11:02	36.30	80.00	673.00	3.20	1253.00	12.60	4.36	14.00	374.00	0.00	374.00	46.00
5/14/02	11:03	34.90	80.00	675.00	3.20	1097.00	12.20	4.36	15.00	367.00	0.00	367.00	54.00
	Average	42.25	79.92	627.17	3.11	1077.75	13.13	3.93	13.33	358.33	1.50	359.92	32.08
	Stdv	7.44	0.29	52.86	0.09	354.40	0.65	0.51	0.98	8.42	1.57	7.56	12.40

Results from A&M Co-fire project 7 **May 14-17, 2002**
Gas Analyzer results

Low phosphorus manure blended 90/10

Date	Time	Combust Efficiency	Ambient Temp	Stack Temp	O2 %	CO ppm	CO2 %	Combustibles	Excess air	Nitric oxide	Nitrogen dioxide	NOX	SOX
5/15/02	11:31	44.90	80.00	485.00	3.90	1086.00	14.20	4.36	16.00	369.00	3.00	373.00	22.00
5/15/02	11:32	41.70	81.00	589.00	3.80	1328.00	13.90	4.36	15.00	381.00	0.00	381.00	35.00
5/15/02	11:34	40.10	81.00	666.00	3.60	971.00	14.00	4.36	15.00	382.00	0.00	382.00	48.00
5/15/02	11:35	39.80	80.00	693.00	3.50	1340.00	14.00	4.36	14.00	379.00	0.00	379.00	44.00
5/15/02	11:36	38.60	80.00	712.00	3.50	1156.00	13.80	4.36	14.00	387.00	0.00	387.00	48.00
5/15/02	11:37	37.30	81.00	724.00	3.40	1183.00	13.40	4.36	14.00	387.00	0.00	387.00	52.00
5/15/02	11:38	36.00	81.00	735.00	3.40	1380.00	13.00	4.36	15.00	391.00	0.00	391.00	52.00
5/15/02	11:39	35.50	81.00	744.00	3.50	1169.00	13.00	4.36	15.00	394.00	0.00	394.00	53.00
5/15/02	11:40	34.10	81.00	748.00	3.60	936.00	12.60	4.36	16.00	399.00	0.00	399.00	50.00
5/15/02	11:41	33.50	81.00	750.00	3.70	971.00	12.40	4.36	17.00	401.00	0.00	401.00	45.00
5/15/02	11:42	33.00	82.00	755.00	3.60	788.00	12.30	4.36	17.00	404.00	0.00	404.00	54.00
5/15/02	11:43	31.50	81.00	761.00	3.50	1049.00	11.90	4.36	17.00	400.00	0.00	400.00	53.00
5/15/02	11:44	31.30	81.00	765.00	3.50	866.00	11.90	4.36	17.00	407.00	0.00	407.00	55.00
	Average	36.72	80.85	702.08	3.58	1094.08	13.11	4.36	15.54	390.85	0.23	391.15	47.00
	Stdv	4.15	0.55	81.32	0.15	186.50	0.83	0.00	1.20	11.25	0.83	10.64	9.26

Results from A&M Co-fire project 7 **May 14-17, 2002**
Gas Analyzer results

Low phosphorus manure blended 90/10

Date	Time	Combust Efficiency	Ambient Temp	Stack Temp	O2 %	CO ppm	CO2 %	Combustibles	Excess air	Nitric oxide	Nitrogen dioxide	NOX	SOX
5/16/02	11:49	37.30	83.00	663.00	2.50	1897.00	12.80	4.36	11.00	343.00	0.00	343.00	62.00
5/16/02	11:51	34.60	84.00	698.00	2.60	1828.00	12.20	4.36	12.00	348.00	0.00	348.00	69.00
5/16/02	11:52	45.00	84.00	713.00	2.40	1864.00	11.90	3.50	11.00	343.00	0.00	343.00	67.00
5/16/02	11:53	44.30	84.00	725.00	2.50	1774.00	11.80	3.21	12.00	352.00	0.00	352.00	62.00
5/16/02	11:54	29.50	84.00	731.00	2.70	1673.00	11.00	4.07	14.00	356.00	0.00	356.00	61.00
5/16/02	11:55	28.00	84.00	739.00	2.30	2087.00	10.70	4.36	12.00	342.00	0.00	342.00	52.00
5/16/02	11:56	26.50	84.00	744.00	2.20	2847.00	10.40	4.36	12.00	344.00	0.00	344.00	53.00
5/16/02	11:57	24.50	85.00	747.00	2.30	2060.00	10.00	4.36	13.00	351.00	0.00	351.00	72.00
5/16/02	11:58	22.20	85.00	754.00	2.40	1912.00	9.60	4.36	14.00	359.00	0.00	359.00	67.00
5/16/02	11:59	21.10	85.00	758.00	2.40	2075.00	9.40	4.36	15.00	354.00	0.00	354.00	62.00
5/16/02	12:00	19.10	85.00	762.00	2.40	2276.00	9.10	4.36	15.00	354.00	0.00	354.00	57.00
5/16/02	12:01	18.00	85.00	767.00	2.40	2151.00	9.00	4.36	15.00	357.00	0.00	357.00	64.00
5/16/02	12:02	16.50	85.00	771.00	2.30	2160.00	8.80	4.36	15.00	351.00	0.00	351.00	64.00
	Average	28.20	84.38	736.31	2.42	2046.46	10.52	4.18	13.15	350.31	0.00	350.31	62.46
	Stdv	9.55	0.65	30.70	0.13	296.53	1.34	0.38	1.57	5.81	0.00	5.81	5.85

Results from A&M Co-fire project 7 **May 14-17, 2002**
Gas Analyzer results

High phosphorus manure blended 90/10

Date	Time	Combust Efficiency	Ambient Temp	Stack Temp	O2 %	CO ppm	CO2 %	Combustibles	Excess air	Nitric oxide	Nitrogen dioxide	NOX	SOX
5/17/02	11:12	55.90	80.00	407.00	3.90	1190.00	14.00	3.21	16.00	258.00	0.00	258.00	17.00
5/17/02	11:13	54.80	80.00	473.00	3.60	1157.00	14.20	3.21	15.00	258.00	0.00	258.00	22.00
5/17/02	11:14	54.60	80.00	519.00	3.40	1197.00	14.50	3.21	13.00	258.00	0.00	258.00	32.00
5/17/02	11:15	53.50	80.00	549.00	3.20	1303.00	14.30	3.21	13.00	258.00	0.00	258.00	41.00
5/17/02	11:16	52.60	80.00	571.00	3.20	1386.00	14.10	3.21	13.00	260.00	0.00	260.00	56.00
5/17/02	11:17	52.60	80.00	588.00	3.10	1300.00	14.30	3.21	12.00	261.00	0.00	261.00	63.00
5/17/02	11:18	51.50	80.00	599.00	3.10	1304.00	13.80	3.21	13.00	262.00	0.00	262.00	66.00
5/17/02	11:19	51.80	80.00	608.00	3.10	1228.00	14.10	3.21	13.00	264.00	0.00	264.00	76.00
5/17/02	11:20	51.20	80.00	616.00	3.10	1432.00	13.90	3.21	13.00	267.00	0.00	267.00	75.00
5/17/02	11:21	51.00	80.00	621.00	3.00	1382.00	13.80	3.21	12.00	266.00	0.00	266.00	75.00
5/17/02	11:22	51.00	80.00	629.00	3.10	1303.00	14.00	3.21	13.00	268.00	0.00	268.00	82.00
5/17/02	11:23	50.40	80.00	634.00	3.00	1339.00	13.70	3.21	12.00	267.00	0.00	267.00	77.00
5/17/02	11:24	50.50	80.00	639.00	3.10	1408.00	13.80	3.21	13.00	270.00	0.00	270.00	80.00
	Average	52.42	80.00	573.31	3.22	1302.23	14.04	3.21	13.15	262.85	0.00	262.85	58.62
	Stdv	1.79	0.00	69.85	0.26	88.05	0.24	0.00	1.14	4.38	0.00	4.38	23.01

Results from A&M Co-fire project 7 **May 14-17, 2002**
Gas Analyzer results

High phosphorus manure blended 90/10

Date	Time	Combust Efficiency	Ambient Temp	Stack Temp	O2 %	CO ppm	CO2 %	Combustibles	Excess air	Nitric oxide	Nitrogen dioxide	NOX	SOX
5/17/02	14:43	61.30	80.00	463.00	4.80	554.00	12.30	2.08	22.00	295.00	0.00	295.00	41.00
5/17/02	14:44	60.70	79.00	477.00	4.80	545.00	12.20	2.08	23.00	298.00	0.00	298.00	42.00
5/17/02	14:45	48.90	80.00	487.00	4.70	594.00	11.90	3.21	23.00	295.00	0.00	295.00	46.00
5/17/02	14:46	48.00	80.00	500.00	4.90	667.00	11.80	3.21	24.00	304.00	0.00	304.00	50.00
5/17/02	14:47	47.90	80.00	508.00	4.70	610.00	11.80	3.21	23.00	300.00	0.00	300.00	48.00
5/17/02	14:48	47.30	80.00	515.00	4.70	598.00	11.60	3.21	24.00	302.00	0.00	302.00	45.00
5/17/02	14:49	46.50	80.00	521.00	4.80	568.00	11.40	3.21	24.00	305.00	0.00	305.00	44.00
5/17/02	14:50	45.90	80.00	523.00	4.80	553.00	11.20	3.21	25.00	307.00	0.00	307.00	41.00
5/17/02	14:51	45.70	80.00	529.00	4.90	555.00	11.20	3.21	25.00	308.00	0.00	308.00	48.00
5/17/02	14:52	45.00	80.00	535.00	4.90	505.00	11.10	3.21	26.00	307.00	0.00	307.00	47.00
5/17/02	14:53	45.10	80.00	539.00	4.90	564.00	11.10	3.21	25.00	308.00	0.00	308.00	44.00
5/17/02	14:54	56.30	80.00	543.00	4.90	505.00	10.80	2.93	26.00	313.00	0.00	313.00	44.00
	Average	49.88	79.92	511.67	4.82	568.17	11.53	3.00	24.17	303.50	0.00	303.50	45.00
	Stdv	5.99	0.29	25.46	0.08	44.94	0.47	0.44	1.27	5.62	0.00	5.62	2.89

Results from A&M Co-fire project 7 **May 14-17, 2002**
Gas Analyzer results

Low phosphorus manure blended 90/10

	Combust Efficiency	Ambient Temp	Stack Temp	O2 %	CO ppm	CO2 %	Combustibles	Excess air	Nitric oxide	Nitrogen dioxide	NOX	SOX
Average test 1	42.25	79.92	627.17	3.11	1077.75	13.13	3.93	13.33	358.33	1.50	359.92	32.08
Average test 2	36.72	80.85	702.08	3.58	1094.08	13.11	4.36	15.54	390.85	0.23	391.15	47.00
Average test 3	28.20	84.38	736.31	2.42	2046.46	10.52	4.18	13.15	350.31	0.00	350.31	62.46
Average	35.72	81.72	688.52	3.03	1406.10	12.25	4.16	14.01	366.50	0.58	367.13	47.18
Stdv	7.08	2.36	55.82	0.58	554.63	1.50	0.22	1.33	21.47	0.81	21.36	15.19

High phosphorus manure blended 90/10

	Combust Efficiency	Ambient Temp	Stack Temp	O2 %	CO ppm	CO2 %	Combustibles	Excess air	Nitric oxide	Nitrogen dioxide	NOX	SOX
Average test 1	52.42	80.00	573.31	3.22	1302.23	14.04	3.21	13.15	262.85	0.00	262.85	58.62
Average test 2	49.88	79.92	511.67	4.82	568.17	11.53	3.00	24.17	303.50	0.00	303.50	45.00
Average	51.15	79.96	542.49	4.02	935.20	12.79	3.10	18.66	283.17	0.00	283.17	51.81
Stdv	1.79	0.06	43.59	1.13	519.06	1.77	0.15	7.79	28.75	0.00	28.75	9.63

Ash and Water samples analyzed for levels of Phosphorus

Following the advice from Huffman laboratories Inc., gas from the boiler was bubbled through a 0.01 molar solution of sodium hydroxide. This procedure could allow the phosphorus to precipitate into the solution and make phosphorus gas analyzing possible. The sample was bubbled through 500 ml of the solution of NaOH for 20 minutes at 20 CF/hour. A total of 5 cubic feet of air was bubbled through the solution. The solution had a pH 12 in de-ionized water. The samples were then analyzed by Inductively Coupled Plasma Atomic Emission Spectroscopy method (ICP-AES) and the results are as follows:

Date	Fuel blend	Results
5/15/2002	Low P	<0.2 mg/L phosphorus
5/16/2002	Low P	<0.2 mg/L phosphorus
5/17/2002	High P	<0.2 mg/L phosphorus
5/17/2002	High P	<0.2 mg/L phosphorus
5/15/2002	Blank	<0.2 mg/L phosphorus

All samples tested for phosphorus concentrations were lower than the detection limits.

An ash sample was collected after each experiment and analyzed for phosphorus and nitrogen content. The results are as follows:

Date	Sample type	Dry basis Nitrogen (ppm)	Dry basis Phosphorus (ppm)
5/15/2002	Low P	10945.1	21264.76
	Low P	10317.4	23720.38
	Mean +/-stdv	10631.25 +/-443.85	22492.57 +/-1736.39
5/16/2002	Low P	7894.554	26475.27
	Low P	7207.009	30397.56
	Mean +/-stdv	7550.78 +/-486.17	28436.42 +/-2773.48
5/17/2002	Low P	12200.79	19621.9
	Low P	13045.54	20542.97
	Mean +/-stdv	12623.17 +/- 597.33	20082.43 +/-651.29
5/17/2002	High P	7899.4	33024.91
	High P	8933.847	30750.73
	Mean +/-stdv	8416.62 +/-731.46	31887.82 +/-1608.09
5/14/2002	High P	8092.866	21282.9
	High P	9540.546	20301.92
	Mean +/-stdv	8816.71 +/-1023.66	20792.41 +/-693.66

kh

Appendix B: Fixed Bed Gasification (Task 3)

Parametric studies were conducted for all the types of fuel under two primary air flow rates: 45 and 60 SCFH. It is necessary to perform the experiments under different airflow rates in order to study the affect of airflow rate on the gasification rate for different fuels. The fuel size was further classified into two groups, 1) 0.5" < $D_{particle}$ <0.25", and 2) 0.25" < $D_{particle}$ <0.157". The fuel was classified into two groups in order to study the particle size effect on the process dynamics. As mentioned in the previous report (quarterly report 7) during the experiments the bed height was maintained constant at 6.75"±0.5" above the grate. All the experiments were started in a similar fashion, by preheating the set up to 500°F, and then adding 300gm of fuel and continuing the heating process until the temperature in the bottom of the bed reached up to 1500°F, after which the external heating in the plenum chamber was stopped and more fuel was slowly added to obtain the required bed height. After obtaining the required bed height, the temperature readings were recorded at every three-minute interval, and the gas samples were collected from the six sampling ports. Table 3.1 shows the status of the experiments for different fuels under conditions. The experiments for coal, feedlot biomass (FB), and coal and feedlot biomass blends (CFB) have been completed. The experiments for chicken litter biomass (LB), and coal and chicken litter biomass blends (CLB) are in progress. The experiments with soil surfaced feedlot biomass (SSFB) are yet to be started. The blends are always in a ratio of 50:50 percent by weight of both the fuels.

S.No.	Fuel Type	PA = 45 SCFH, SA = 0 SCFH		PA = 60 SCFH, SA = 0 SCFH	
		Temp Profile	Gas composition	Temp Profile	Gas composition
1	Coal	Y	Y	Y	Y
2	Coal (2)	Y	Y	Y	Y
3	FB	Y	Y	Y	Y
4	FB (2)	Y	Y	Y	Y
5	LB	Y	N	N	N
6	LB (2)	Y	N	N	N
7	CFB	Y	Y	Y	Y
8	CFB (2)	Y	Y	Y	N
9	CLB	Y	N	N	N
10	CLB (2)	Y	N	N	N
11	SSFB	N	N	N	N
12	SSFB (2)	N	N	N	N
13	CSSFB	N	N	N	N
14	CSSFB (2)	N	N	N	N

Table 3.1: Status (as on 7/7/02) of experiments for different fuels.

Assuming a single film model for carbon burning and using the concept of electrical circuit analog the ratio of the kinetic and diffusion resistances shall enable to determine whether the burning is kinetic controlled or otherwise.

$$\frac{R_{kin}}{R_{diff}} = \left(\frac{n_I}{n_I + Y_{O_2,S}}\right)\left(\frac{R_u T_S}{MW_{mix} P}\right)\left(\frac{r D}{k_c}\right)\left(\frac{1}{r_S}\right)$$

$C + O_2 \rightarrow CO_2$

$$n_I = \frac{31.99}{12.01} = 2.664,$$

Assuming:

$$Y_{O_2,S} = 0, MW_{mix} = 30 {}^{kJ}\!/_{kmol}, k_c = 13.9 m/s$$

Let Ts = 1500K

$$r = \frac{P}{\left(\frac{R_u}{MW_{mix}}\right)T_S} = \frac{100}{\left(\frac{8.314}{30}\right)1500} = 0.24 kg/m^3$$

$$D = \left(\frac{1500}{393}\right)^{1.5} 1.6 * 10^{-5} = 1.19 * 10^{-4} m^2/s$$

Particle size (in)	R_{kin}/R_{diff}	Remark
0.157	0.0021419	$R_{kin} << R_{diff}$, Diffusion controlled
0.25	0.0013451	$R_{kin} << R_{diff}$, Diffusion controlled
0.5	0.0006725	$R_{kin} << R_{diff}$, Diffusion controlled

From the above table it can be concluded that burning of char is mostly diffusion controlled, which implies that the burning rate is dependent on the amount of surface area available for the reaction. The $S_{V,p}$ ratio, which is the ratio of the surface area of each particle to its volume, gives some interesting explanations for the temperature profile in the bed.

$$S_{V,p} = \left(\frac{Surface \quad Area}{Volume}\right) = \frac{3}{a}$$

$$S_{V,bed} = n'''\left(4\pi a^2\right) = \frac{6}{\pi a^3}\frac{\pi a^2}{} = \frac{6}{a}$$

$$\Rightarrow S_{V,bed} = 2S_{V,p}$$

It means that, as the particle size increases the $S_{V,bed}$ ratio (i.e. less number of particles per unit volume) as well as the $S_{V,p}$ decreases, and effective surface area available per unit volume of the reactor (also the effective surface area per unit volume of the particle) decreases. Thus, the reaction rate decreases resulting in lower peak temperatures in the bed, longer residence time for the attaining the same carbon conversion, and the movement of the oxidation zone towards the free surface. The decreased burning rate causes the oxygen to penetrate further into the bed (i.e. towards the free surface), thus causing the movement of the oxidation zone towards the free surface.

1. Temperature profiles:

Consider the following discussion on the temperature profile variation in the bed: Three consecutive cells, *i-1*, *i*, and *i+1*, are control volumes (refer to the figure shown in the following page), across which an energy balance shall yield some interesting results.

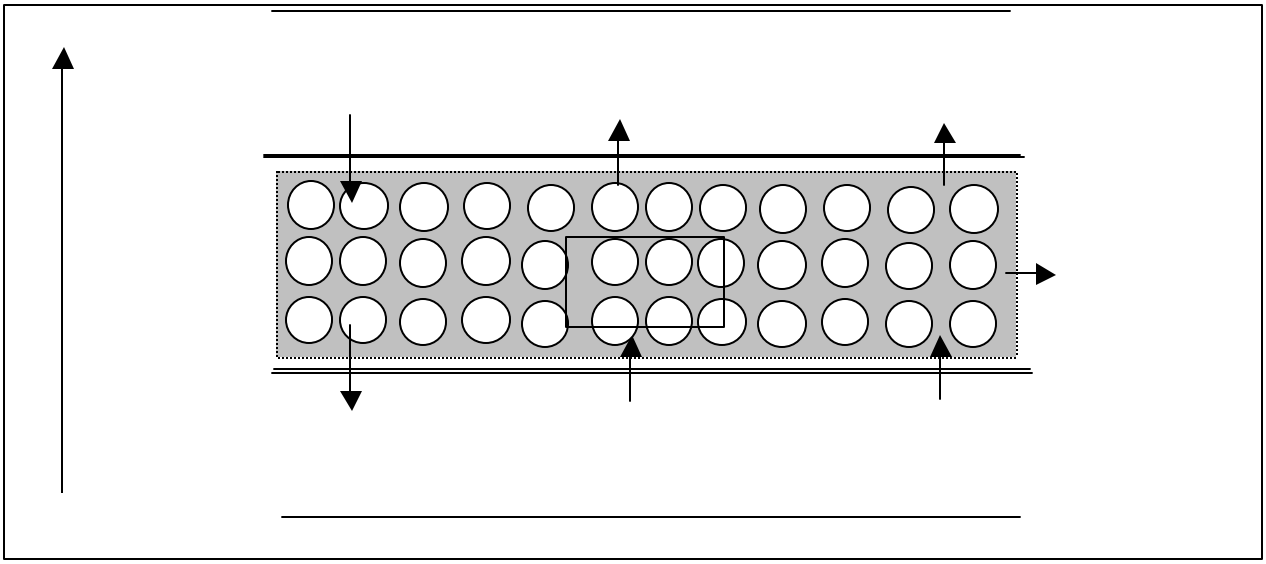

In

$\dot{m}_{fuel,in,i+1} c_{p,fuel} T_{gas,out,i} + \dot{m}_{gas,in,i-1} c_{p,gas,T_{g,i-1}} T_{gas,in,i-1}$

Out

$\dot{m}_{fuel,out,i} c_{p,fuel} T_{gas,in,i-1} + \dot{m}_{gas,out,i} c_{p,gas,T_{g,i}} T_{gas,out,i}$

Generation

$\dot{m}_{chem,hetro,i} h_c - \dot{m}_{pyro} h_{pyro} - \dot{m}_{evap} h_{fg}$

Simplification:

$\dot{m}_{gas,out,i} = \dot{m}_{gas,in,i-1} + \dot{m}_{chem,hetro,i}$

$\dot{m}_{fuel,out,i} = \dot{m}_{gas,in,i-1} - \dot{m}_{chem,hetro,i}$

Energy Balance gives:

$E_{in} + E_{gen} = E_{out}$

$$\dot{m}_{gas,in,i-1}\left(c_{p,gas,T_{g,i}} T_{gas,out,i} - c_{p,gas,T_{g,i-1}} T_{gas,in,i-1} \right) = \dot{m}_{fuel,in,i+1} c_{p,fuel} \left(T_{gas,out,i} - T_{gas,in,i-1} \right) + \dot{m}_{chem,hetro}\left(h_c + c_{p,fuel} T_{gas,in,i-1} - c_{p,gas,T_{g,i}} T_{gas,out,i} \right) - \dot{m}_{pyro} h_{pyro} - \dot{m}_{evap} h_{fg}$$

when $\dot{m}_{chem,hetro} = 0$, *then the above equation reduces to*:

$$\dot{m}_{gas,in,i-1}\left(c_{p,gas,T_{g,i}} T_{gas,out,i} - c_{p,gas,T_{g,i-1}} T_{gas,in,i-1} \right) = \dot{m}_{fuel,in,i+1} c_{p,fuel} \left(T_{gas,out,i} - T_{gas,in,i-1} \right) - \dot{m}_{pyro} h_{pyro} - \dot{m}_{evap} h_{fg}$$

$\therefore$ $T_{gas,out,i} - T_{gas,in,i-1}$ *is small, So* $T_{gas,out,i} \approx T_{gas,in,i-1}$

i.e. in the region in which there is no heterogeneous reaction, then the temperature is low.

However, when there is heterogeneous reaction, then:
$T_{gas,out,i} >> T_{gas,in,i-1}$, So there is a peak temperature in the bed, and beyond this region, the heterogeneous reaction is very slow or not occurring at all. This causes the average temperature beyond the peak to fall rapidly in the bed. The above discussion is a very simplified model, in which the inter particle heat transfer due to conduction, and radiation have not been considered. In addition, the convective heat exchange between the two phases has also not been considered. The heat transfer due to conduction might not cause the temperature gradient in the bed to be so steep, especially near the peak temperature region (oxidation front). The assumptions involved in the above model are that:

1. The gas phase average temperature and the solid phase average temperature are equal.
2. The specific heat of the solid phase is constant through out the bed.
3. The heat loss through the sidewalls is negligible.
4. The heat transfer due to conduction and radiation has been neglected.

The temperature profiles for coal, feedlot biomass, and CFB shall be discussed below.

1.1. Effect of Air flow rate:

The temperature profiles for different airflow rates were obtained for the above-mentioned fuels.

1.1a. Coal:

Figures 1a and 1b shows the comparative temperature profiles in the bed for various fuel particle sizes under different air flow rates. For coal, it is observed that the peak temperature in the bed occurs at the bottom of the bed. As the air flow rate is increased from 45 SCFH to 60 SCFH, the peak temperature at the base of the bed is lowered. This is due to two reasons,

a) Faster accumulation of ash at the bottom of the bed due to higher burn rate of fuel.
b) Higher air flow rate results in more sensible heat loss from the bed.
c) More fuel added to attain the initial bed height, resulting in higher mass in the bed, thus increasing the heat sink capacity of the bed (refer figure A). It also provides an increased char mass in the bed, which might increase the burn rate. So if effect (b) dominates effect (c), then the temperature can decrease.

For larger particle sizes ($0.25" < D_p < 0.5"$), at t=60 min at PA= 60 SCFH (refer figure 1a), the temperature at the base of the bed decreases and there is a peak shift, implying that ash accumulation at the base results in lower combustibles at the base thus decreasing the temperature at the base. As air flow rate increases, the ash accumulation rate increases due to increase in the burn rate.

For smaller particle sizes ($0.157" < D_p < 0.25"$) as the air flow rate increases the peak temperature at the bottom of bed decreases (refer figure 1b), this is due to the same reasons as explained for larger sized particles. However, the temperature profiles in the bed are similar for both the air flow rates. Thus showing that, for small particles the air flow rate doesn't affect the temperature profile to a distinguishable degree. This might be due to a negligible effect of Reynolds number on the heat transfer coefficient.

1.1b. Feedlot Biomass:

Figures 2a and 2b shows the comparative temperature profiles in the bed for various fuel particle sizes under different air flow rates. There is a distinct difference in the profile from that of coal. In this case, there is a distinct peak in the bed. To explain this we look at the design of the gasifier and the fuel properties. Table 1 shows a comparative study of the fuel properties for both coal and feedlot biomass. The fixed carbon in feedlot biomass is only 17.33% where as its

41.92% for coal, where as the volatile matter is about 57% for feedlot biomass and 32.58% for coal. Since studies have found that the pyrolysis temperature of feedlot about 100 degrees lower than that of coal. This implies that the feedlot particle shall be almost char by the time it enters the oxidation zone, though the same might not be true for coal. So it is clear for a given particle size of feedlot and coal, the feedlot particle shall burn faster, due to lower fixed carbon, higher volatile matter and lower pyrolysis temperature. Also higher the volatile matter, more the porosity of the particle, thus feedlot biomass is expected to be more porous compared to coal. This can be further qualitatively shown from the Thiele modulus, which depends on the diffusivity in the pore, rate constant of reaction, pore dimension, and external surface concentration.

$$f = L_P\left(\frac{kCs^{m-1}}{V_p D}\right)^{1/2},$$

Where,
L_P = effective pore length = r/3 for spheres
k = reaction rate constant
C_S = external surface concentration
M = reaction order
V_P = pore volume
D = diffusivity

The average reaction rate within the particle may be related to the rate based on the surface concentrations in terms of the effectiveness factor, which is defined as follows:

$$h = \frac{(r')}{\left(r'_{c=c_s}\right)} = \frac{Tanhf}{f}$$, for an isothermal particle.

So when $\phi \rightarrow$ zero, $\eta \rightarrow 1$ meaning that $r = r_{cs}$. Under these conditions, all the pore area is accessible for the reaction. However, when $\phi \rightarrow \infty$, $\eta \rightarrow 0$ meaning that the reaction is exclusively at the particle external surface and the reactant gas does not penetrate into the pores.

Proximate Analysis				Ultimate Analysis			
	Feedlot	**Coal**	**Feedlot (high ash)**	**Element**	**Feedlot**	**Coal**	**Feedlot (high ash)**
Dry loss	10.875	21.225	6.16	**Carbon**	37.205	56.345	18.225
Volatile Matter	56.965	32.58	30.155	**Hydrogen**	5.65	5.905	3.03
Fixed Carbon	17.33	41.92	7.26	**Oxygen by difference**	38.26	32.35	20.065
Ash	14.83	4.275	56.325	**Nitrogen**	3.405	0.85	1.845
Phosphorus	0.955		0.955	**Sulfur**	0.65	0.275	0.41
HHV (BTU/Lb)	6441.5	9376	2984	**Ash**	14.83	4.275	56.325

Table 1: Fuel analysis

Assume, that the particles at the bottom of the bed are mostly char in both cases for feedlot as well as for coal. Also, assume that the reaction rate constants are approximately equal for the two chars. Since the feedlot biomass has higher volatile matter than coal, so for the post pyrolysis regime the feedlot biomass char is more porous than the coal char, which means that the pore volume is higher in feedlot biomass than coal, i.e. higher internal surface area for feedlot

biomass as compared to coal. This means that the reactivity of feedlot char is greater than that of coal, so feedlot char shall burn faster than coal char under similar (diffusion controlled) conditions.

The gasifier grate design does not permit the removal of ash from the bottom of the bed during operations. So due to the greater ash content in feedlot biomass, coupled with a higher rate of burning as compared to coal and a lower fixed carbon in the feedlot biomass the lower portion in the bed is primarily ash in the case of feedlot biomass. This leads to a lowering of temperature at the bottom of the bed and so the peak temperature moves up i.e., the oxidation zone moves towards the free surface. So as time progresses, the peak temperature moves further and further into the bed. This is evident in figure 4. The shift is so apparent as the reactivity of feedlot biomass char is greater than coal and it has lower fixed carbon and most likely a lower ignition temperature.

In order to verify that ash and char reactivity are responsible for the peak temperature shifting in the bed, a similar experiment was done for coal. Figure 1c shows the temperature profile in the bed at one-hour time intervals. It can be clearly observed that the temperature at the bottom of the bed starts to drop slowly and by seven hours into the run, it has dropped by 500K, proving that ash in the fuel is responsible for this particular behavior. The reason it takes such a long time to clearly see such an effect is mainly due to three reasons, a) the ash content in coal is lower than feedlot biomass, b) the fixed carbon content in coal is higher than feedlot biomass, c) the reactivity of coal char is lower than reactivity of feedlot biomass char and d) lower stoichiometric ratio for coal as compared to feedlot biomass. Comparing figures 1c and 2c it can be inferred that the rate of movement of the peak temperature is 3 times faster for feedlot biomass as compared to coal. Figure C shows that the SR for feedlot biomass is around 20% higher than that for coal (0.16) for a primary air flow rate of 45 SCFH. Higher SR implies more oxidizer, i.e., more O_2 is available for combustion, thus a higher reaction rate, resulting in a faster ash accumulation rate, thus a faster shift in the peak temperature.

For larger particle sizes, it is observed that as the air flow rate increases from 45 SCFH to 60 SCFH the peak shift is faster for the higher flow rate (refer figure 2a). From figures C, and D, it is seen that the A/F ratio on a DAF basis is almost similar for both the air flow rates. The faster peak shift results in a higher exit gas temperature.

For smaller sized particles, the peak shift is similar to the larger sized particles, but the peak temperature is about 50K greater than that for the larger sized particles even though the stoichiometric ratios are comparable for both the cases. This may be due to the greater number of fuel particles per unit volume, resulting in a larger surface area per unit volume, thus resulting in a higher peak temperature.

1.1c. <u>Coal: Feedlot biomass blend (50:50 w/w%):</u>

Figures 3a, and 3b show the temperature profiles for coal and feedlot biomass blends. The results confirm the theory of ash and fixed carbon affecting the temperature profile in the bed. It is interesting to note that the temperature at the bottom for CFB fuel is greater than that for feedlot biomass fuel, but lower than that for coal. This is because CFB fuel has lower ash and higher fixed carbon per unit volume as compared to pure feedlot biomass and visa versa as compared to coal. This does not allow the temperature in the bottom of the bed to drop as significantly for CFB fuel as it does for feedlot biomass. The temperature does not drop so much because coal is still burning in the bottom of the bed even though the feedlot biomass has already burnt out. The shifting of the peak temperature is also not clearly present as it was for the feedlot biomass. This is due to coal, which needs a longer residence time to burn, owing to the higher fixed carbon and lower ash content in the fuel. Thus, the peak movement is an indication of ash growth in the bed.

For both larger and smaller sized particles, as the air flow rate increases, the peak temperature increases, and also the peak temperature shift rate also increases. This again is due to a higher burn rate as the amount O_2 supplied increases, and due to an increase in the SR for higher primary air flow rates (refer figure C, and figure D).

1.1d. Chicken Litter Biomass:

Figures 4a, and 4b show the temperature profiles for chicken litter biomass at air flow rate of 45 SCFH. Since, the results of the fuel analysis of litter biomass has not been received, a qualitative discussion shall be discussed for this case. The ash content of litter biomass is estimated to be in the range of 30-35% by mass. The peak shift is significant for both the cases, thus conclusively proving that ash plays a major role in the temperature shift in the bed.

As expected, for coal and litter biomass blends (refer figure 5a, and 5b), the peak-temperature shift rate is slower as compared to coal litter blend. This is due to the same reasons as cited for coal and feedlot biomass blends.

1.2. Effect of Particle size:

The temperature profiles for different fuel particle sizes under the same air flow rates shall be discussed.

1.2a. Coal:

Figures 6a, and 6b show the comparative temperature profiles in the bed for different fuel particle sizes at different air flow rates. For both the cases (PA = 45, and 60 SCFH), the peak temperature for coal particles in the 0.157" to 0.25" range is higher than that of the coal particles in the 0.25" to 0.5" range. This may be due to the higher stoichiometric ratio for smaller coal particles (refer figures C, and D) or more importantly, the S_v ratio for the smaller particles is larger (larger reaction surface area per unit volume) implying a higher burning rate resulting in a higher peak temperature.

The temperature drop in the post pyrolysis region of the bed is greater for smaller particles than that for the larger particles. This is due to the S_V ratio, as in the case of smaller particles a higher S_V ratio implies more mass in the bed, which results in a greater heat sink, thus lowers the temperature in the bed.

1.2b. Feedlot Biomass:

In case of feedlot biomass at primary air flow rate of 45 SCFH, from figure 7a, it can be seen that the peak temperature for both the particle sizes (i.e. $0.157" < D_p < 0.25"$, and $0.25" < D_p < 0.5"$) is almost similar, this may be due to almost similar stoichiometric ratio for both the particle sizes. However, the peak temperature shift is faster for larger sized particles, which may be due to smaller S_V ratio causing the oxidation zone move further towards the free surface.

Interestingly in the case for air flow rate of 60 SCFH, from figure 7b, we see that the peak temperature for smaller sized particles is about 50K higher than that for larger sized particles. This is due to a larger S_V ratio combined with a higher stoichiometric ratio resulting in a higher burning rate thus increasing the peak temperature. However, the peak temperature shift is faster in case of larger sized fuel particles.

1.2c. Coal: Feedlot biomass blend (50:50 w/w%):

The results are along expected lines. Figure 8a, shows that the peak temperature shift is not that significant, confirming our previous observation that ash and fixed carbon affect the peak temperature shift. However, the temperature at the bottom of the bed is always lower for smaller sized particles when compared with larger sized particles. This is due to a higher S_V ratio and a

higher stoichiometric ratio (figure C, and D), which results in a faster burning rate, so the temperature at the bottom decreases faster, due to faster accumulation of ash at the bottom of the bed. The same explanation is applicable for higher air flow rate (refer figure 8b). Though the peak temperature is higher by 100K for air flow rate of 60 SCFH when compared with 45 SCFH. This is due to higher burn rate, due to more availability of O_2 resulting in a higher peak temperature. The higher peak temperature also translates into a faster peak temperature movement towards the free surface.

2. Product Gas composition profile:

Important reactions considered during gasification are:

Heterogeneous Reactions:

C + O2 → CO2 (exothermic) (R1)
C + ½O2 → CO (exothermic) (R2)
C + CO2 → 2CO (Boudouard reaction, endothermic) (R3)
C + H2O → CO + H2 (Water Gas reaction, endothermic) (R4)
C + 2H2 → CH4 (Methanation reaction, exothermic) (R5)

Homogeneous Reactions:

CH4 + 2O2 → CO2 + 2H2O (exothermic) (R6)
H2 + ½O2 --> H2O (exothermic) (R7)
CH4 +H2O --> CO + 3H2 (exothermic) (R8)
CO + ½O2 → CO2 (exothermic) (R9)
CH4 +1/2O2 --> CO + 2H2 (exothermic) (R10)

It is necessary to have an idea about the specific reaction rates of the above-mentioned reactions. For heterogeneous reactions, from figures, 9a, and 9b it can be inferred that in the temperature ranges of 1350K and above the specific rate constant for reaction 2 (R2) shows a rapid increase with Temperature. Thus, at high temperatures CO formation is favored and since under gasification conditions O2 concentration is very small, reaction 2 (formation of CO2) is not that significant. This is of interest as in air gasification CO is the main product gas, and shall enable in interpreting the process dynamics in the gsaifier bed.

In the case of homogeneous reactions, figure, 10a, clearly shows that reaction 7 is the dominant reaction in the gas phase. Though reaction 9 is also fast, but reaction 7 is almost instantaneous, so makes reaction 9 insignificant. Further reaction 8 is faster than reaction 9 and can form CO and H2, and H2 can further react with O2 to produce more water. Reactions 6 and 10 are slow compared to reaction 8 or 9.

2.1.Effect of Air flow rate:

2.1a. Coal:

For smaller sized particles as the air flow rate increases, figure 11 shows that the CO yield at the top of the bed increases by 15% from 25.60% to 29.32%. At the same time, the CO2 also increases by 25%, this is due to an increase in the stoichiometric ratio, as more O2 is available to oxidize CO to CO2. The decrease in fuel feed rate, which decreases by 11% from 20.97 g/min to 18.64 g/min (refer figures E, and F), results in a corresponding decrease in the volatile matter feed rate. The increase in CO might be due to higher temperatures in the bed (in between 3" to 6.57", refer figure 1b), which results in faster pyrolysis of the coal. The increase in CO results in an increase in the HHV (MJ/m3) of the product gas at the top of the bed (refer figure G) by about 6%. Thus, a higher air flow rate is more suitable for smaller sized coal particles, as the HHV of the product gas increases due to an appreciable increase in the CO yield.

For larger sized particles an increase in air flow rate results in an increase in CO2 yield by 71%, thus reducing the increase in CO yield (refer figure 11). The CO yield increases by only 6%, while there is no appreciable increase in H2 yield, where as CH4 yield increases by 23%. The increase in CH4 yield significantly affects the HHV (MJ/m3) of the product gas, which increases by 9.3% (refer figure G). The CO2 increase is significant for larger sized particles due to an increase in the stoichiometric ratio. More importantly as the S_V ratio is less (when compared with smaller sized particles), less char surface area is available for CO is formation, and so as the SR increases the gas phase oxidation of CO to CO2 increases resulting in a significant increase in CO2 yield.

2.1b. Feedlot Biomass:

In case of smaller sized particles figure 12 shows that, an increase in the air flow rate doesn't appreciably change the product gas yield. Thus, the HHV of the product gas does not change much (refer figure G), but decreases by about 4%. The change is not appreciable, as the SR is almost similar for both the air flow rates, thus essentially maintaining the same product gas composition. In addition, though the feed rate increases by 22% from 29.69 g/min to 36.2 g/min (refer figures E, and F) as the air flow rate increases, the product composition might not change due to more significant dilution effect of N2 in the air. The decrease in HHV of the product gas is due to an increase in the CO2 yield along with a decrease in CO, CH4, and H2 yields.

For larger particles, figure 12 shows that the product gas composition does not change appreciably due to an increase in the air flow rate. The HHV of the product gas does not change at all (figure G). This may be due to similar SR for both the air flow rates. More ever, the feed rate decreases by 8% from 39.66 g/min to 36.67 g/min (refer figures E, and F) as the air flow rate increases. So an increase in the CO yield due to higher air flow rate might be counter acted by the dilution effect of N2 in the air, thus keeping the product gas composition almost similar.

2.1c. Coal: Feedlot biomass blend (50:50 w/w%):

In case of larger sized particles, figure 13 shows that as the air flow rate increases, the CO yield increases by 3.5% from 28.07% to 29.03% and H2 yield increases by 11%. Surprisingly the CO2 yield deceases by 20%, and CH4 decreases by 21%. The decrease in CH4 results in a decrease in the HHV of the product gas by 3.3% from 5.2 MJ/m3 to 5.03 MJ/m3 (refer figures G). The feed rate decreases from 30.65 g/min to 24.56 g/min (refer figures E, and F) and the SR increases from 0.14 to 0.23. The temperature in the upper part of the bed (in between 3" to 6.75", refer figure 3a) is higher for higher air flow rate, resulting in more efficient and faster pyrolysis of the fuel, thus increasing the yield of combustible gases. However, this increase is counter acted by the dilution effect of N2, due to an increase in air flow rate followed by an decrease in fuel feed rate.

Since all the experiments have yet to be completed, the detailed discussion about the product-gas composition for different fuels shall be done in the annual report.

1.3.Calculation of burn rate:

Assuming the following:

1. Bed height is constant with respect to time (bed height = 6.75" above the grate).
2. Porosity in the bed is constant with respect to time (ε = constant).
3. Density uniform through out the bed and constant with respect to time (ρ = constant).
4. Ash does not flow out through the grate ($\dot{m}_{ash.bed,out} = 0$).

The average burn rate can be determined as follows:

$$\frac{\partial\left(m_{ash,bed} + m_{comb,bed} + m_{moist,bed}\right)}{\partial t} = 0$$

$$\dot{m}_{ash.bed,out} - \dot{m}_{ash,bed,in} = -\frac{\partial\left(m_{comb,bed} + m_{moist,bed}\right)}{\partial t}$$

$$\dot{m}_{ash,bed,in} = \frac{\partial\left(m_{comb,bed}\right)}{\partial t} = (\dot{m}_{comb,bed,out} - \dot{m}_{comb,bed,in}) + (m_{moist,bed,out} - m_{moist,bed,in})$$

Assu min *g that moisture does'nt react, we have*

$$\dot{m}_{comb,bed,out} = \dot{m}_{ash,bed,in} + \dot{m}_{comb,bed,in} = (1 - Y_{moisture})\,\dot{m}_{fuel}$$

$$\dot{m}_{fuel,burnrate} = \dot{m}_{comb,bed,out} = (1 - Y_{moisture})\,\dot{m}_{fuel}$$

From figure 14, it is seen that as the air flow rate increases the burn rate for all fuels except for FB-(2) and CFB-(2) decrease. For the FB-(2) and CFB-(2) the burn rate increases with an increase in air flow rate.

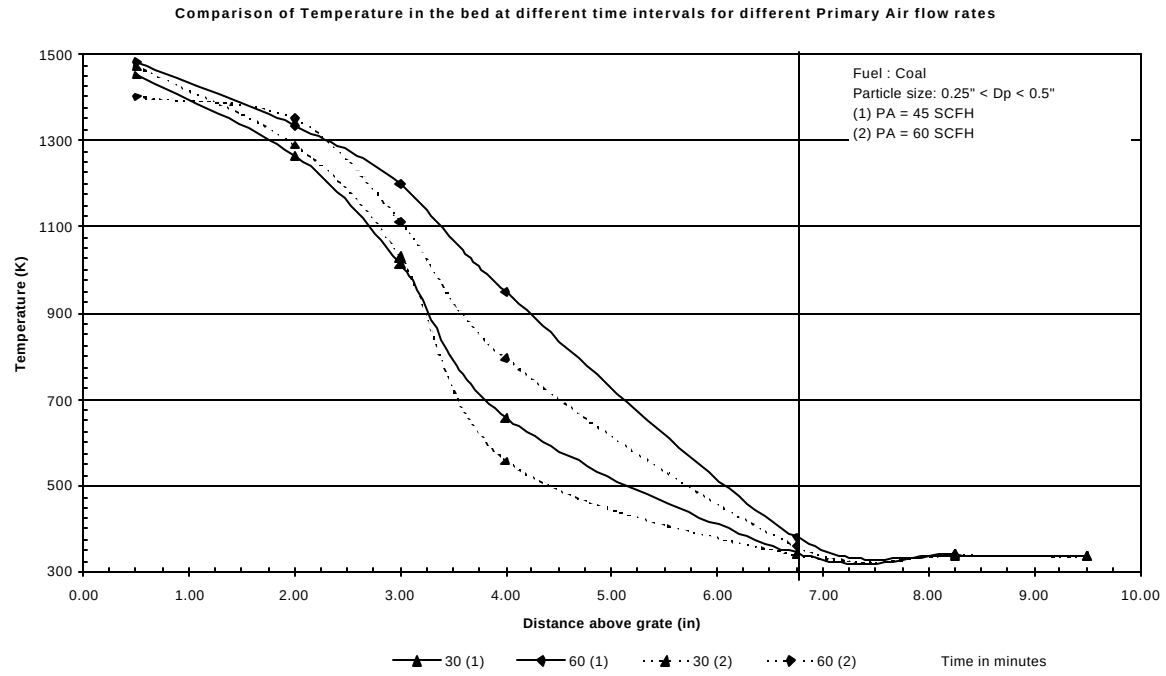

Figure 1a: Comparison of Temperature profiles in the bed for different air flow rates

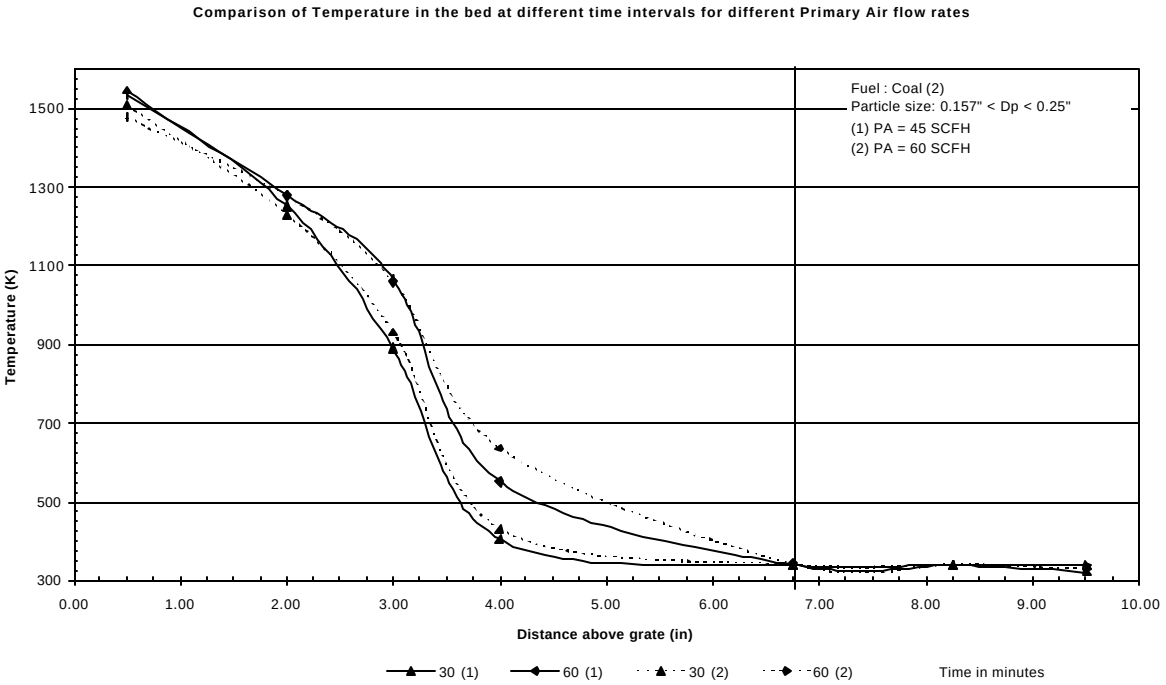

Figure 1b: Comparison of Temperature profiles in the bed for different air flow rates

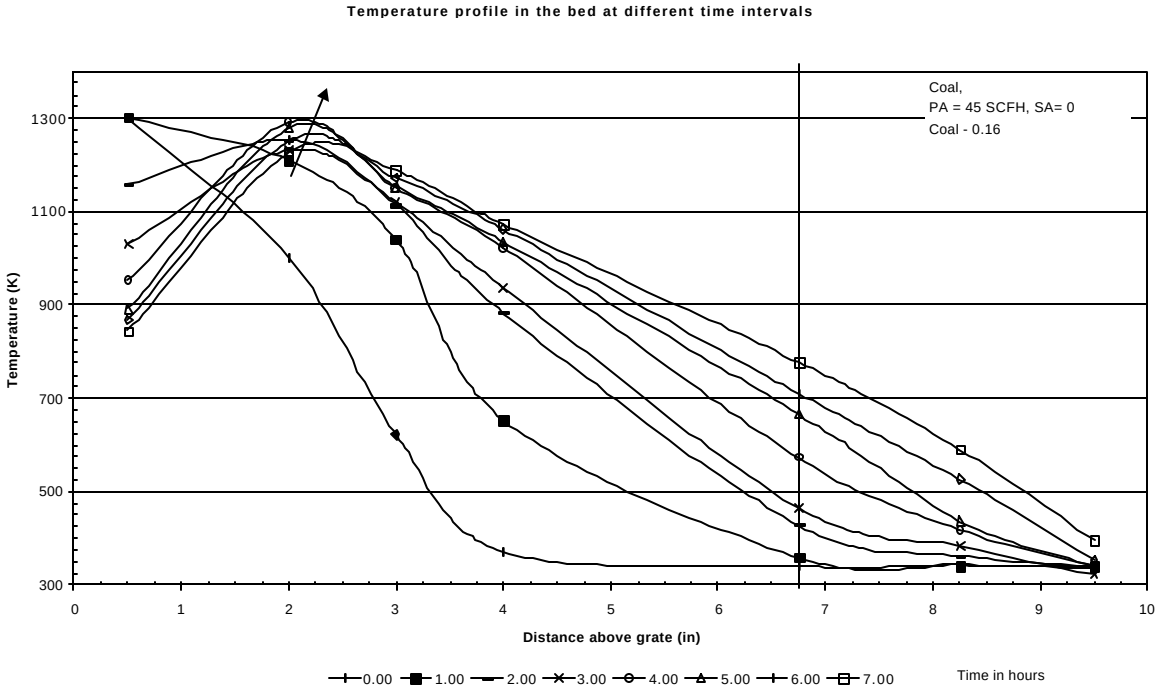

Figure 1c: Temperature profile in the bed at different time intervals.

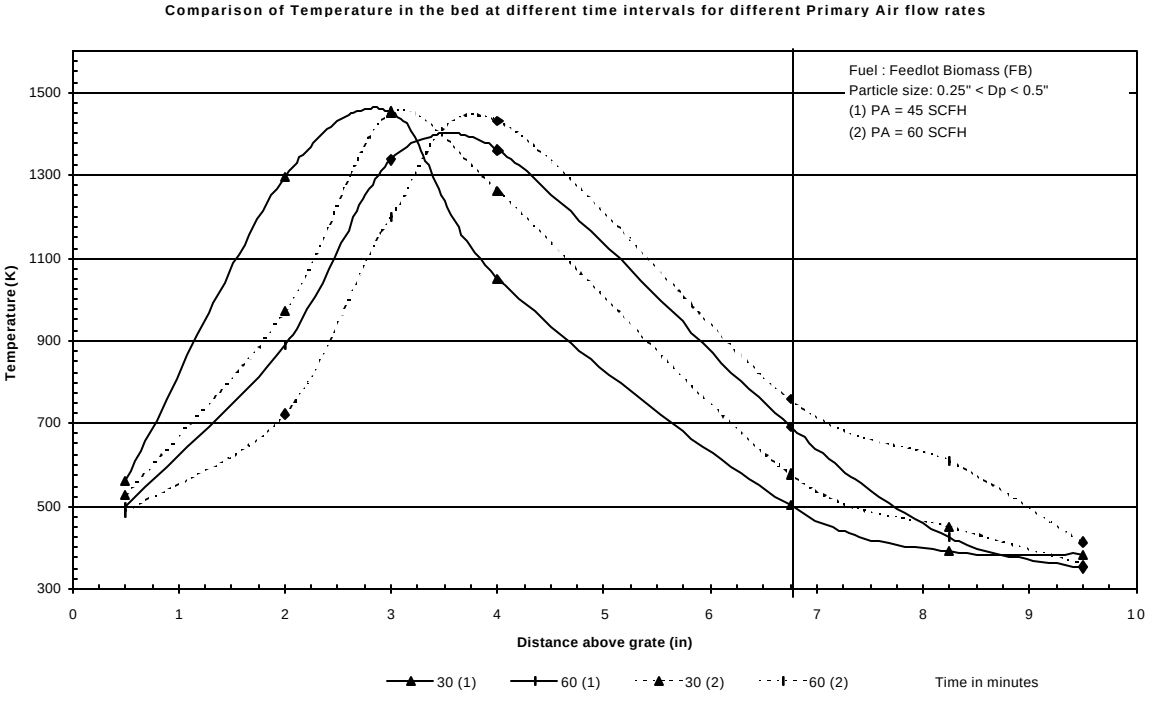

Figure 2a: Comparison of Temperature profiles in the bed for different air flow rates.

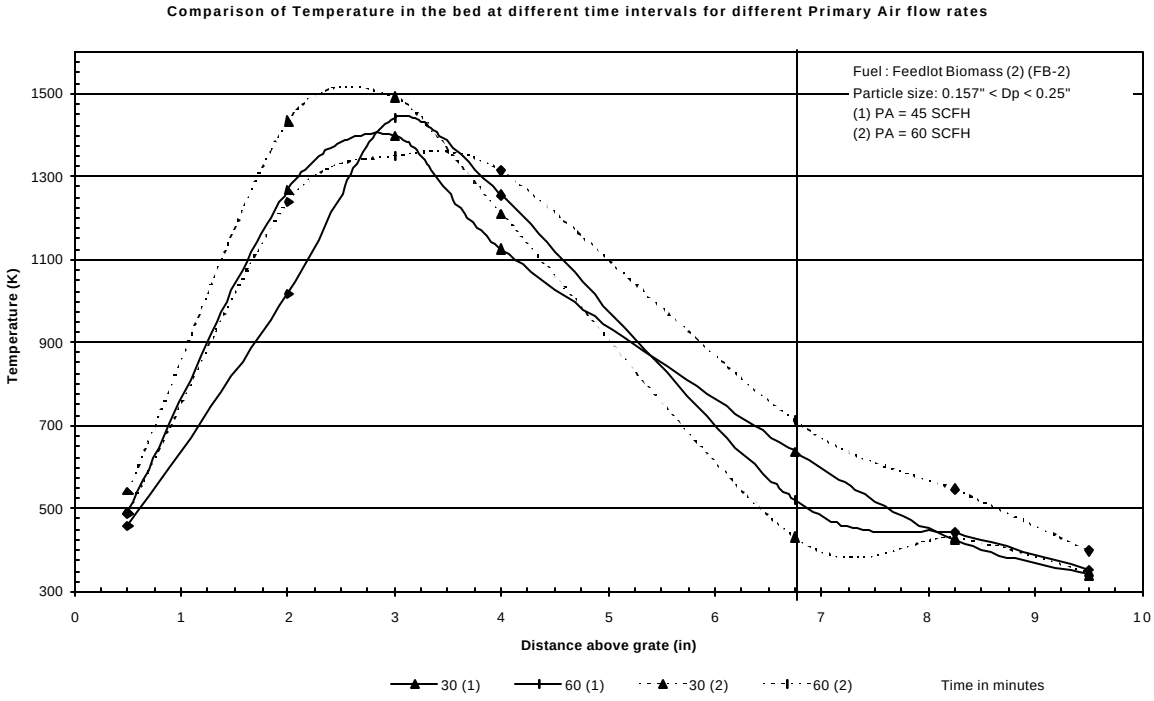

Figure 2b: Comparison of Temperature profiles in the bed for different air flow rates.

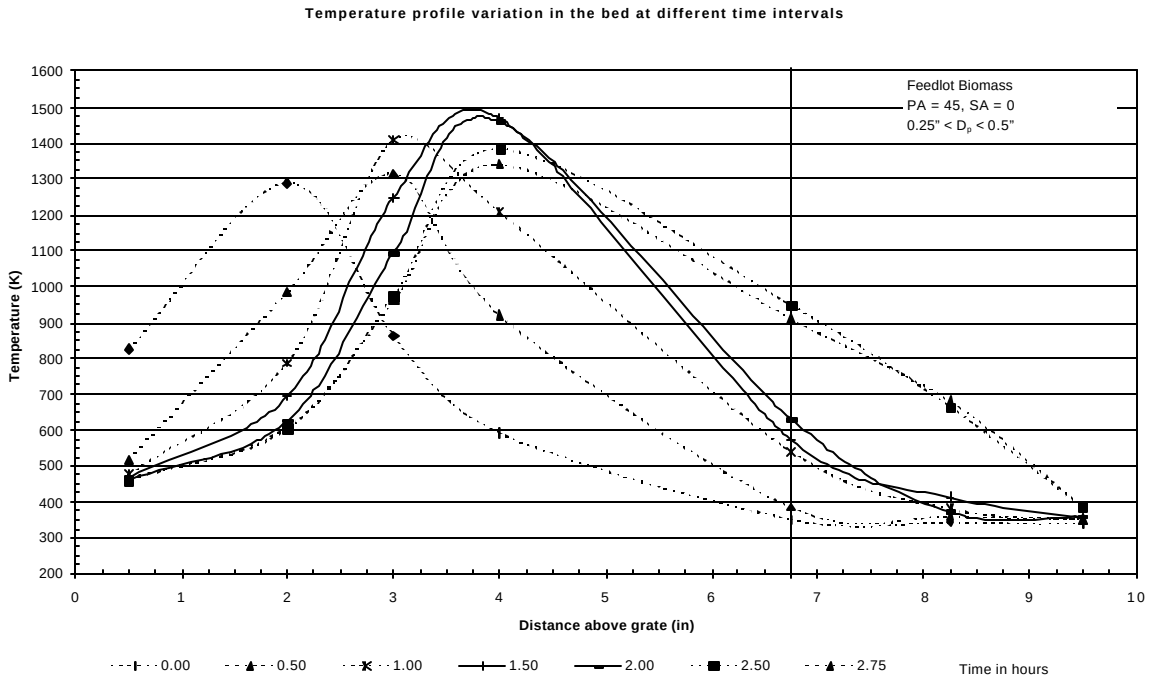

Figure 2c: Temperature profile in the bed at different time intervals.

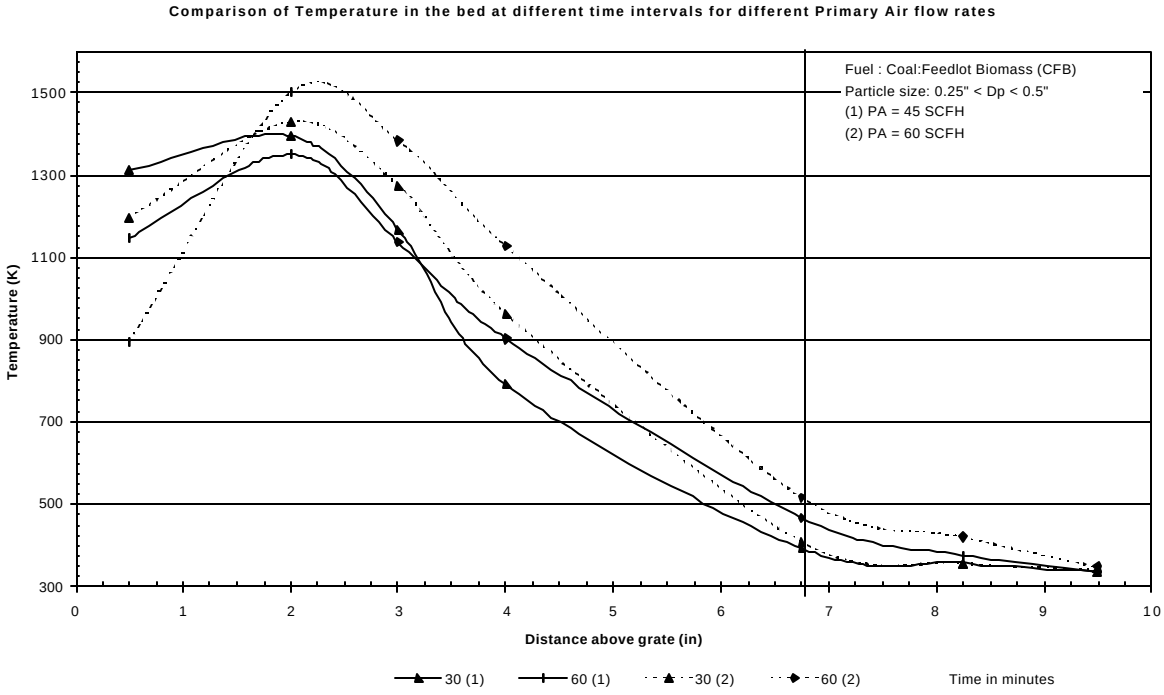

Figure 3a: Comparison of Temperature profiles in the bed for different air flow rates.

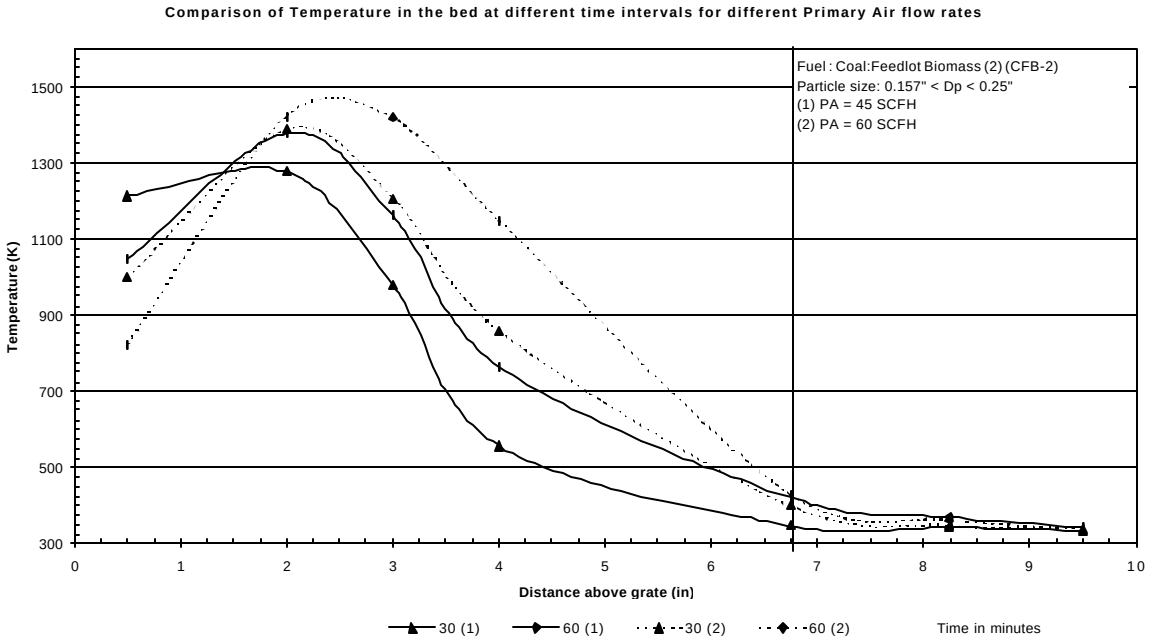

Figure 3b: Comparison of Temperature profiles in the bed for different air flow rates.

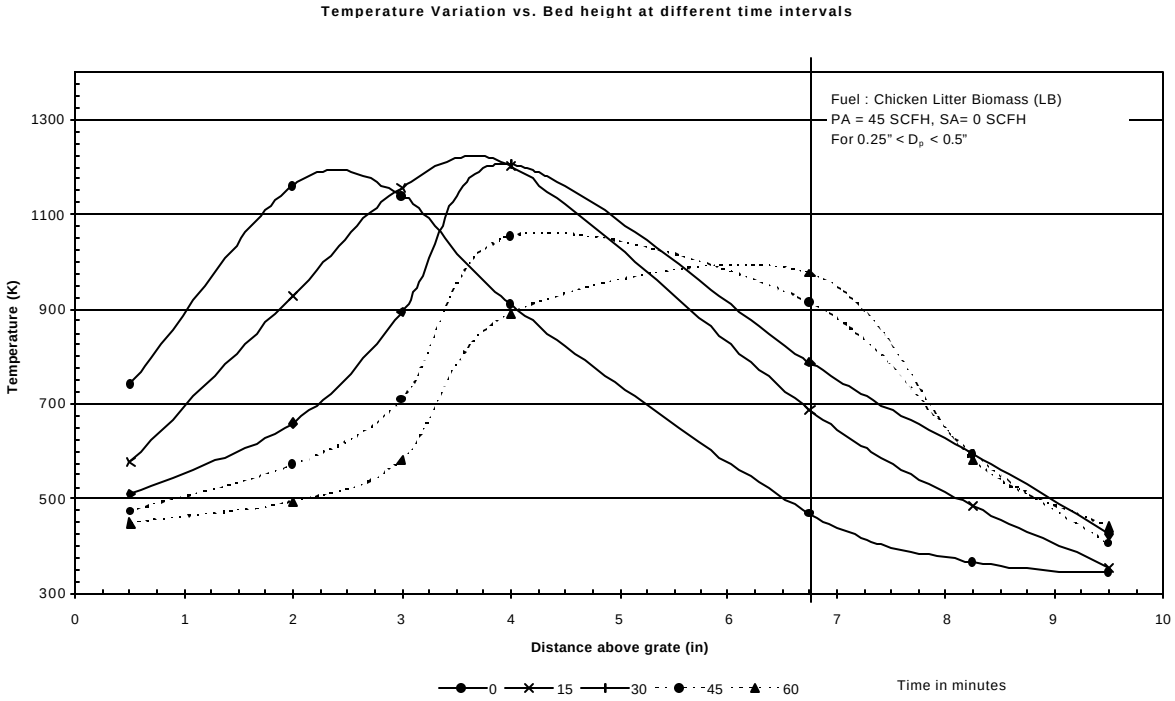

Figure 4a: Temperature profile in the bed for Chicken Litter biomass (LB).

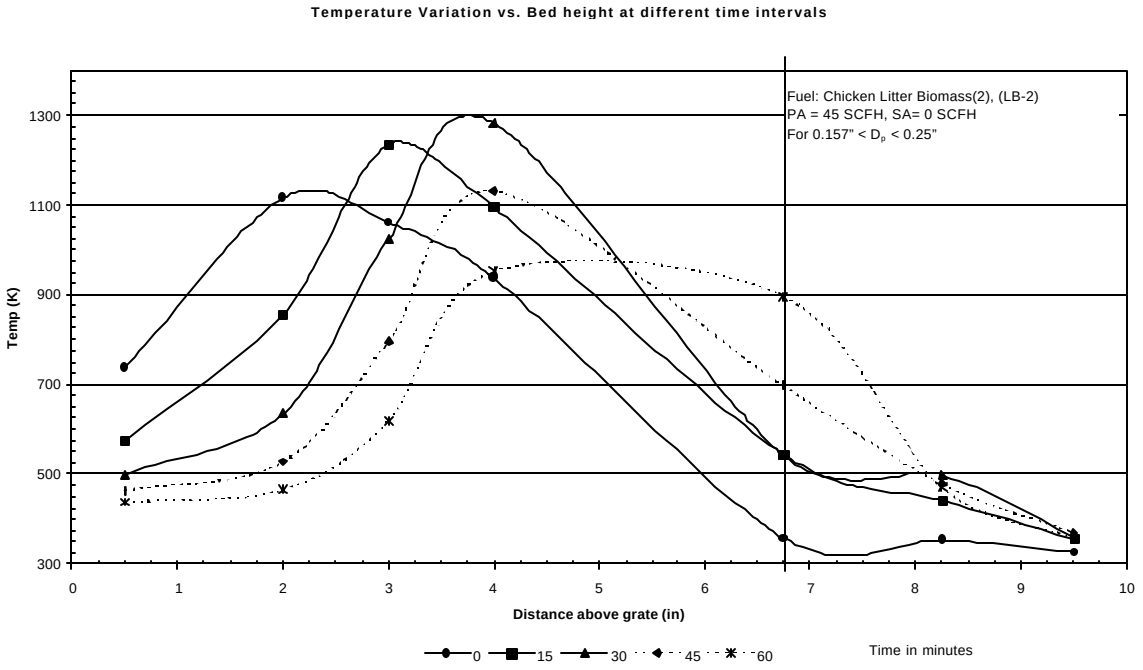

Figure 4b: Temperature profile in the bed for Chicken Litter biomass (LB-2).

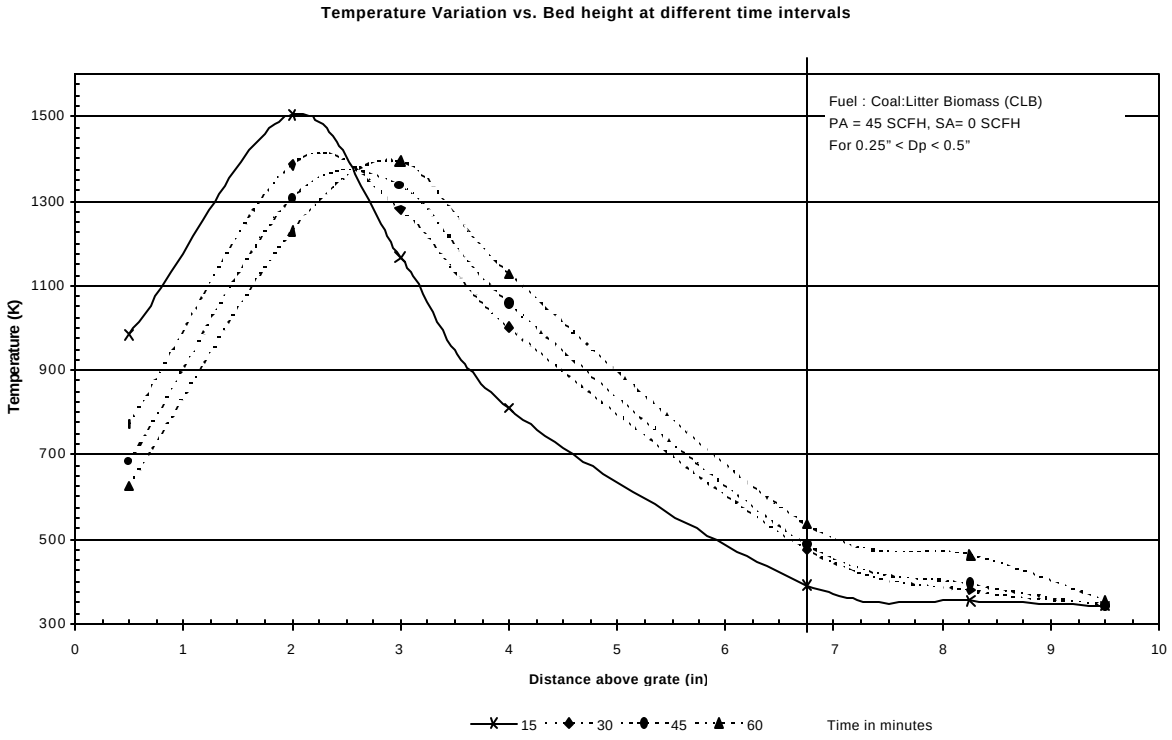

Figure 5a: Temperature profile in the bed for Coal & Chicken Litter biomass Blend (CLB).

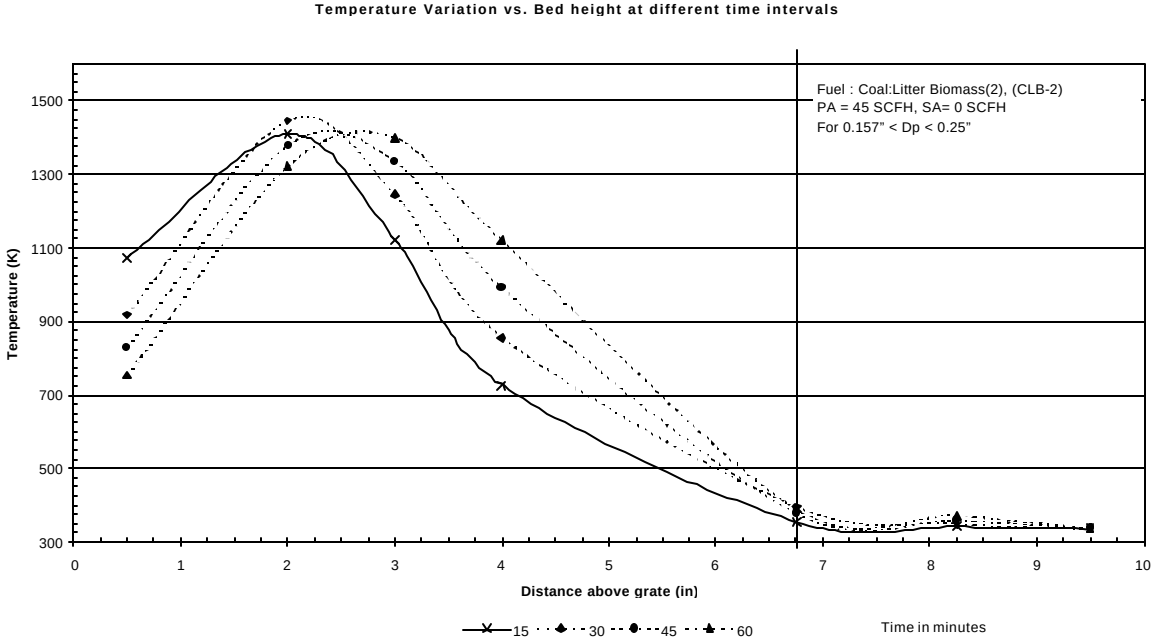

Figure 5b: Temperature profile in the bed for Coal & Chicken Litter biomass Blend (CLB-2).

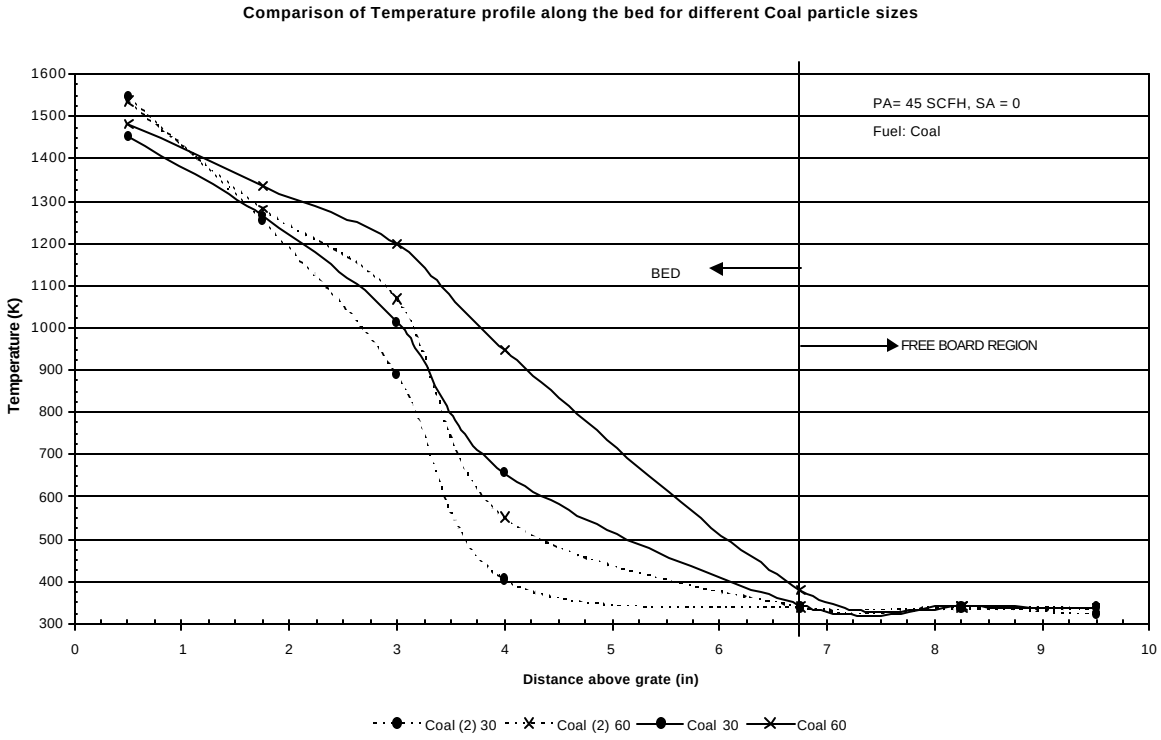

Figure 6a: Comparison of Temperature profile in the bed for different Coal particle sizes.

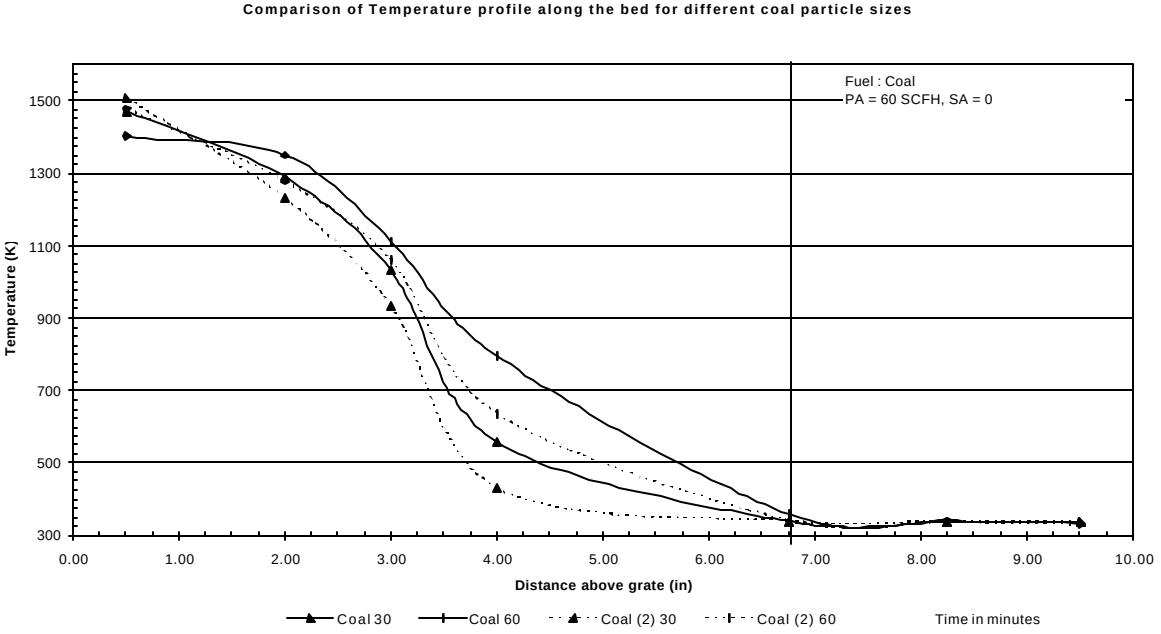

Figure 6b: Comparison of Temperature profile in the bed for different Coal particle sizes.

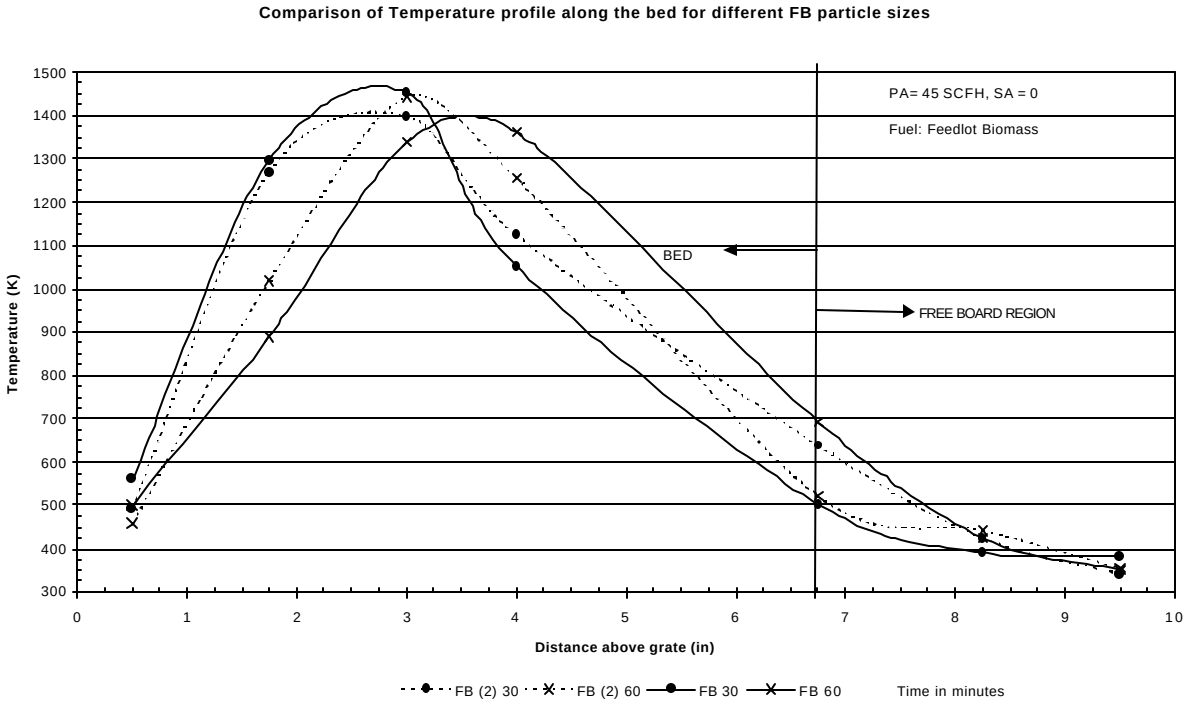

Figure 7a: Comparison of Temperature profile in the bed for different FB particle sizes.

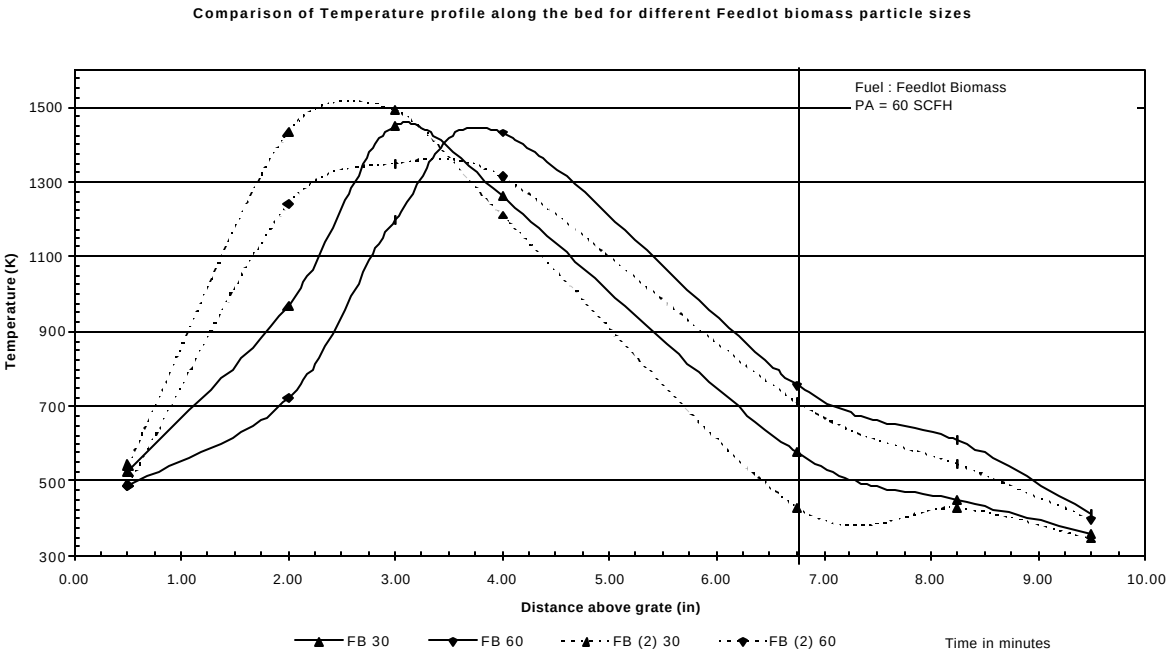

Figure 7b: Comparison of Temperature profile in the bed for different FB particle sizes.

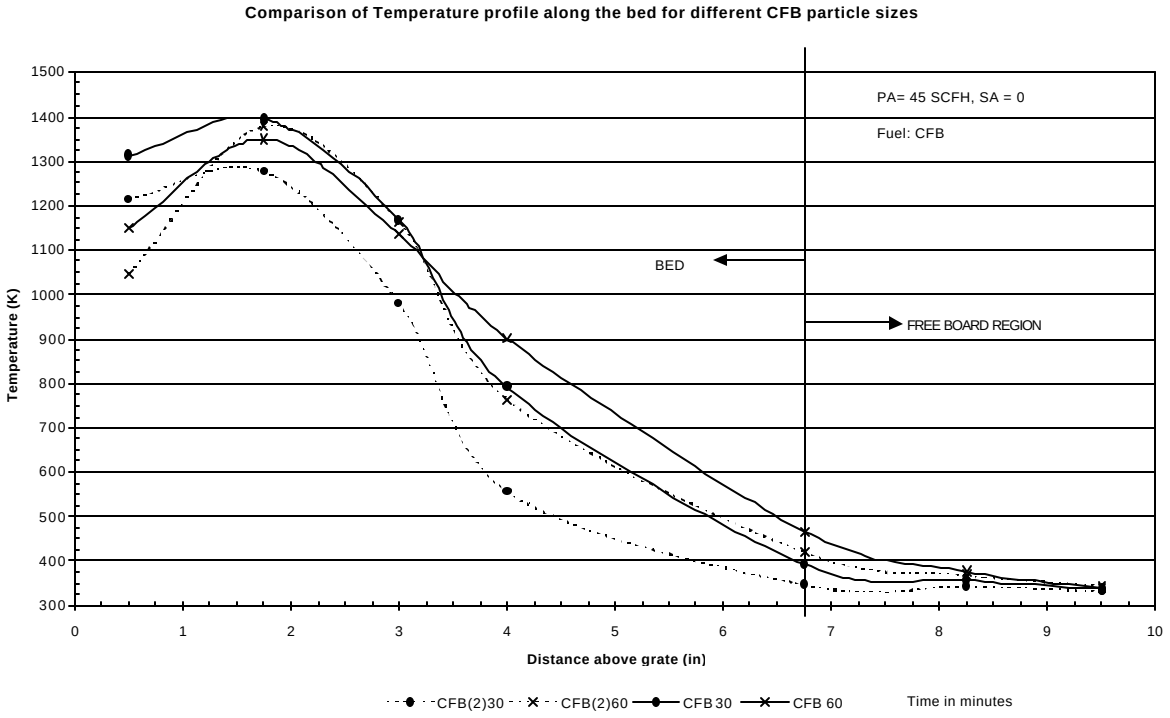

Figure 8a: Comparison of Temperature profile in the bed for different CFB particle sizes.

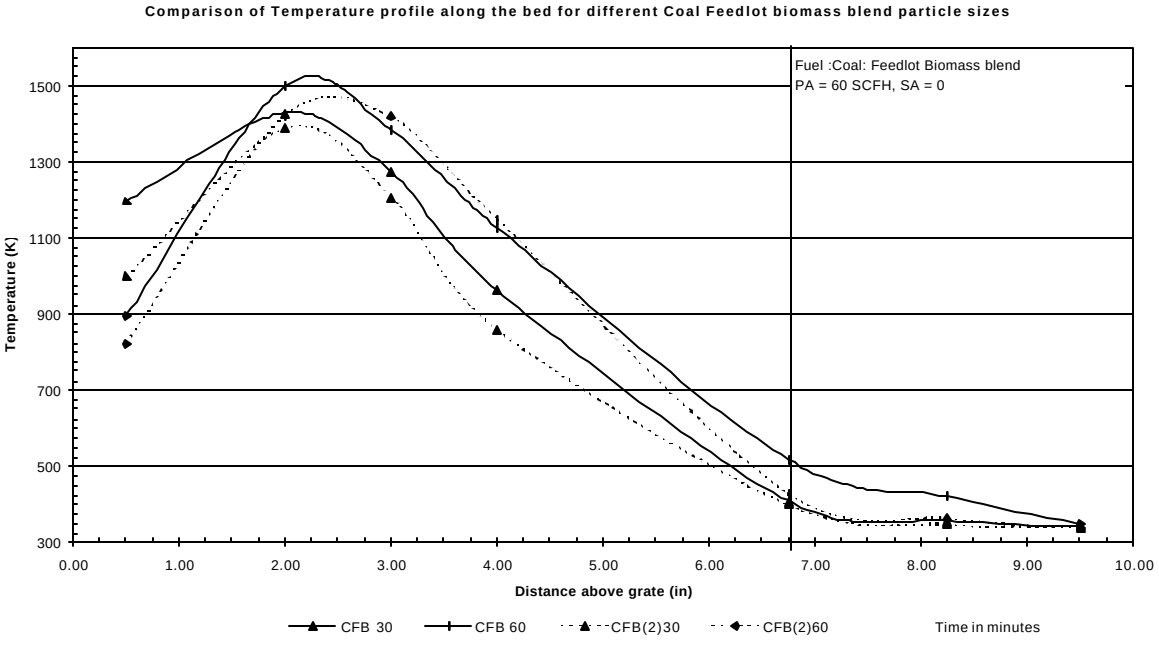

Figure 8b: Comparison of Temperature profile in the bed for different CFB particle sizes.

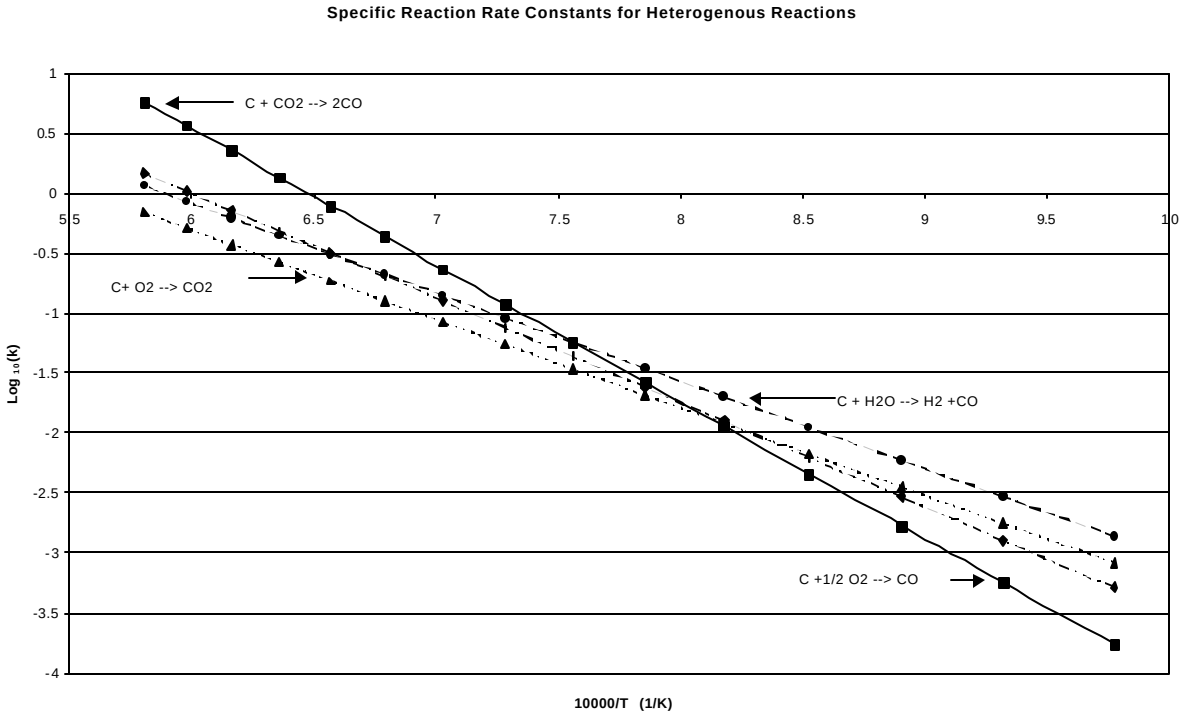

Figure 9a: Specific reaction rate constants for various Heterogeneous Reactions.

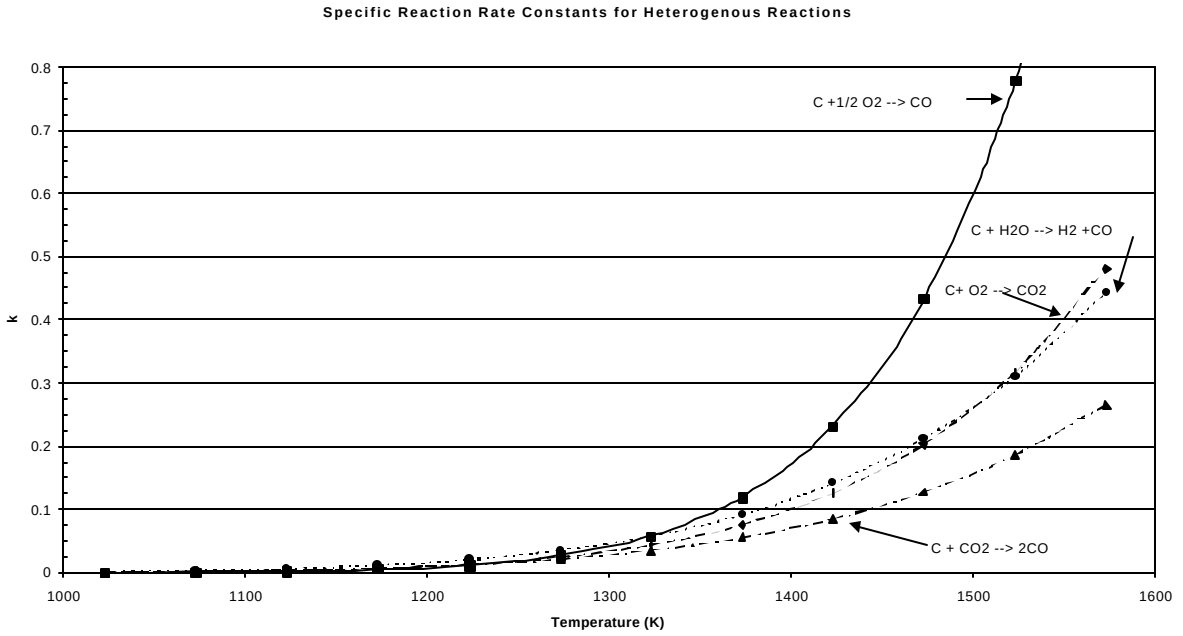

Figure 9b: Variation of Specific reaction rate constants with Temperature for various Heterogeneous Reactions.

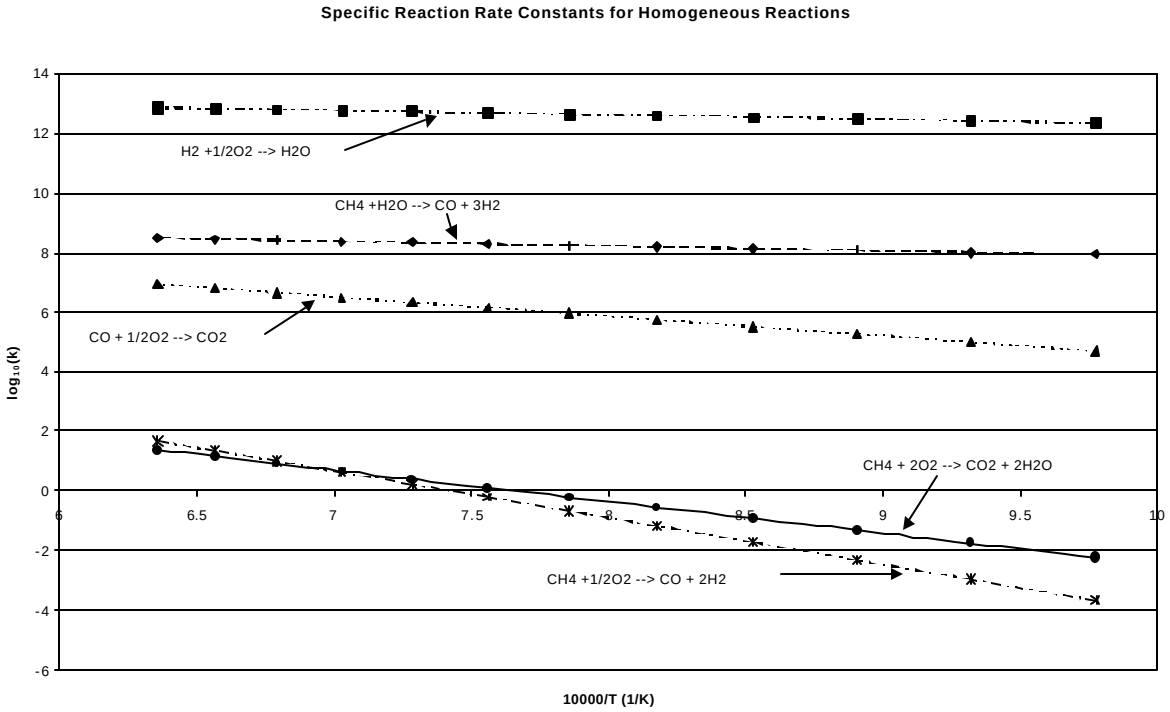

Figure 10a: Specific reaction rate constants for various Homogeneous Reactions.

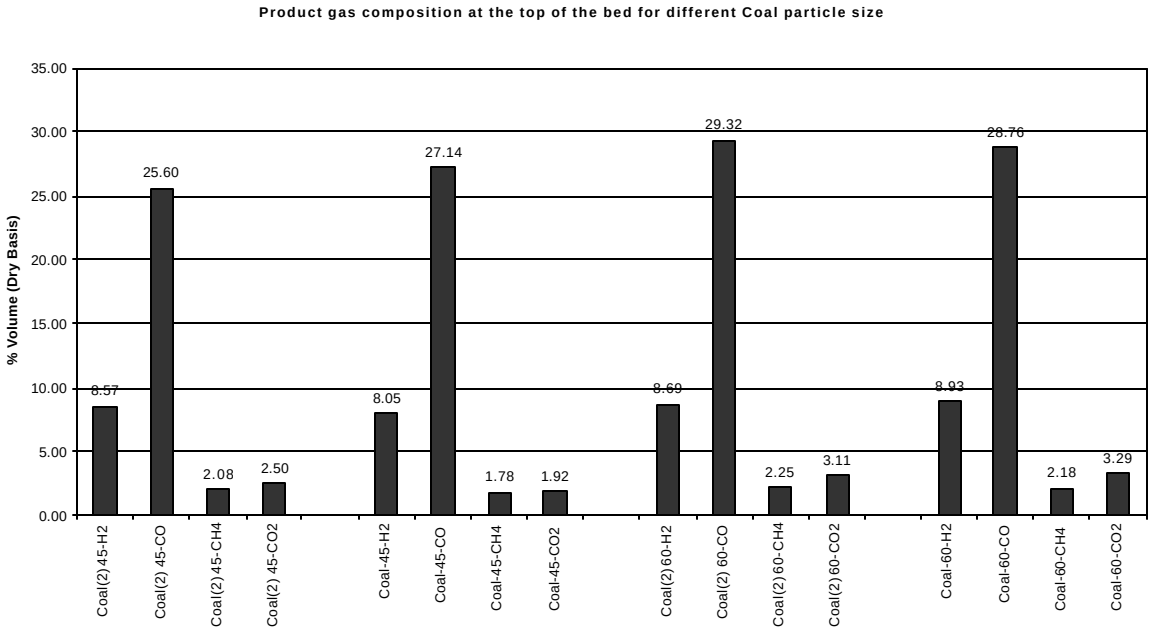

Figure 11: Comparison of product gas composition for coal under different operating conditions.

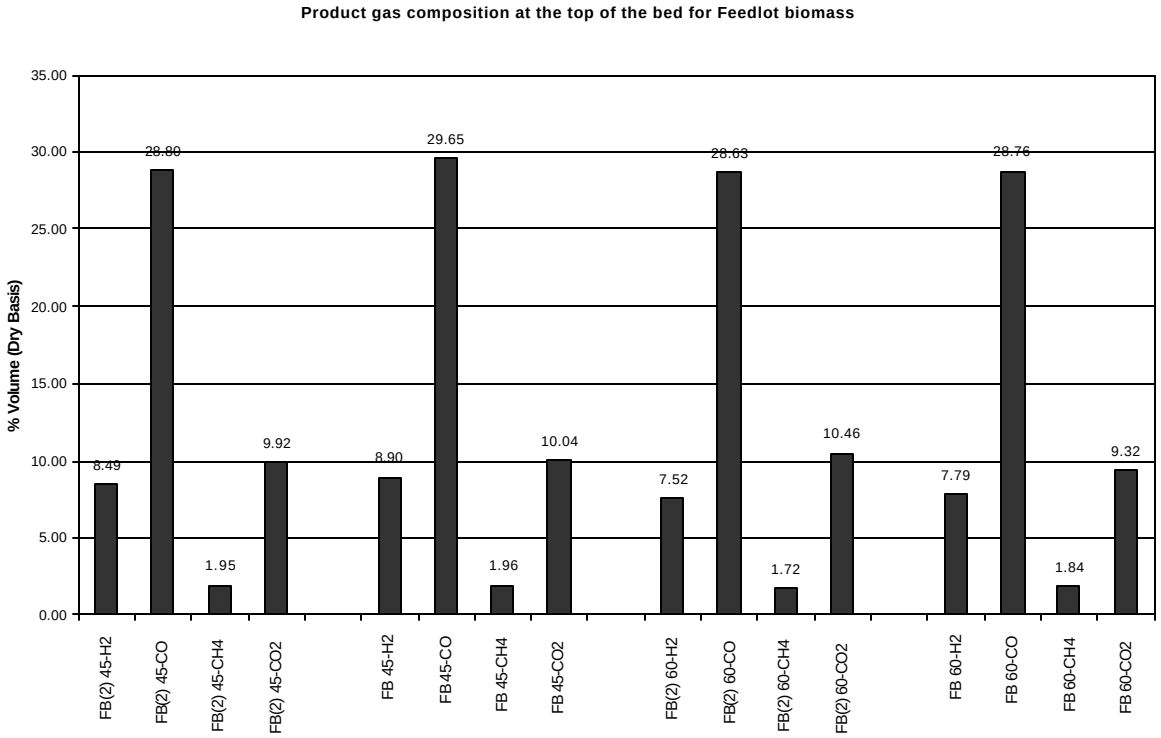

Figure 12: Comparison of product gas composition for FB under different operating conditions.

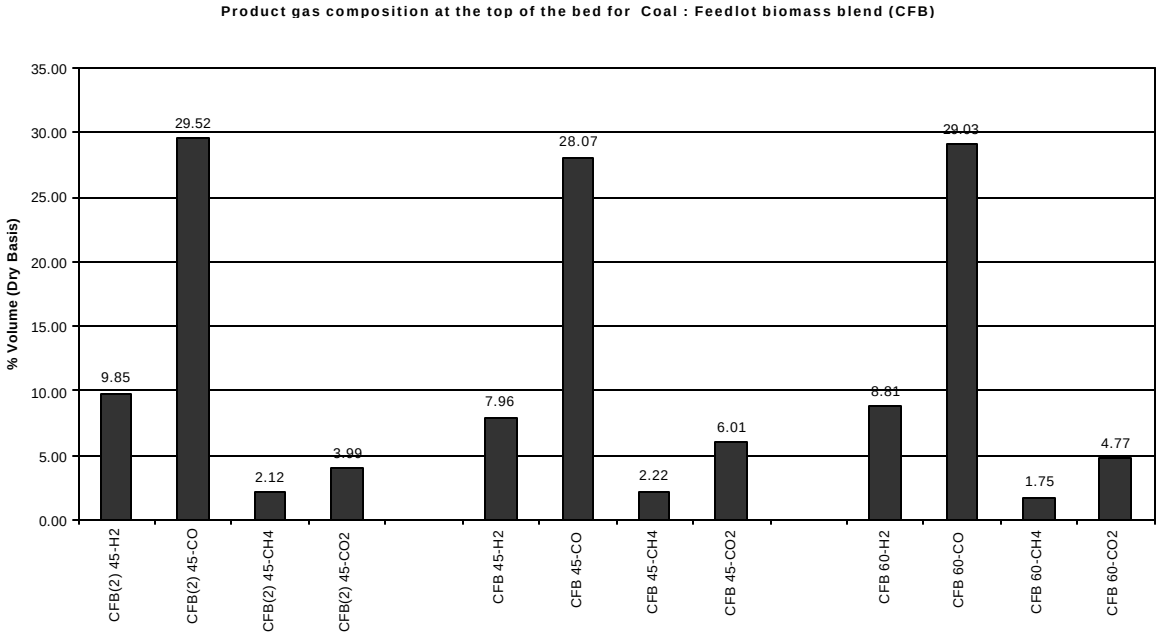

Figure 13: Comparison of product gas composition for CFB under different operating conditions.

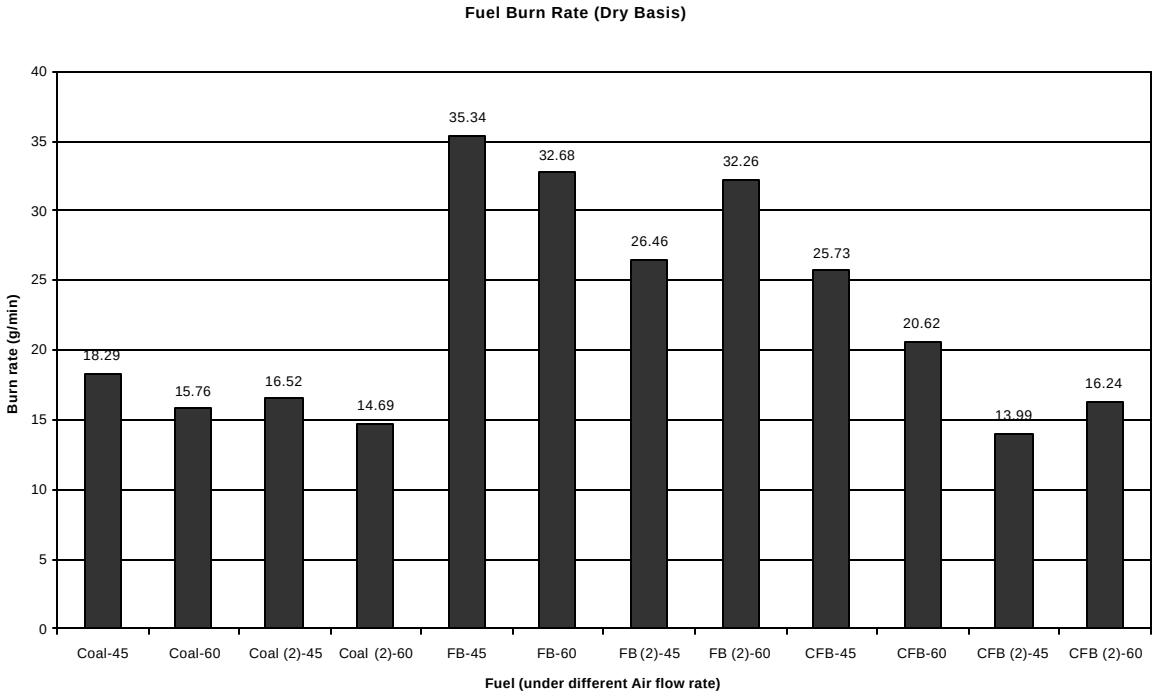

Figure 14: Comparison of burn rate for different fuels.

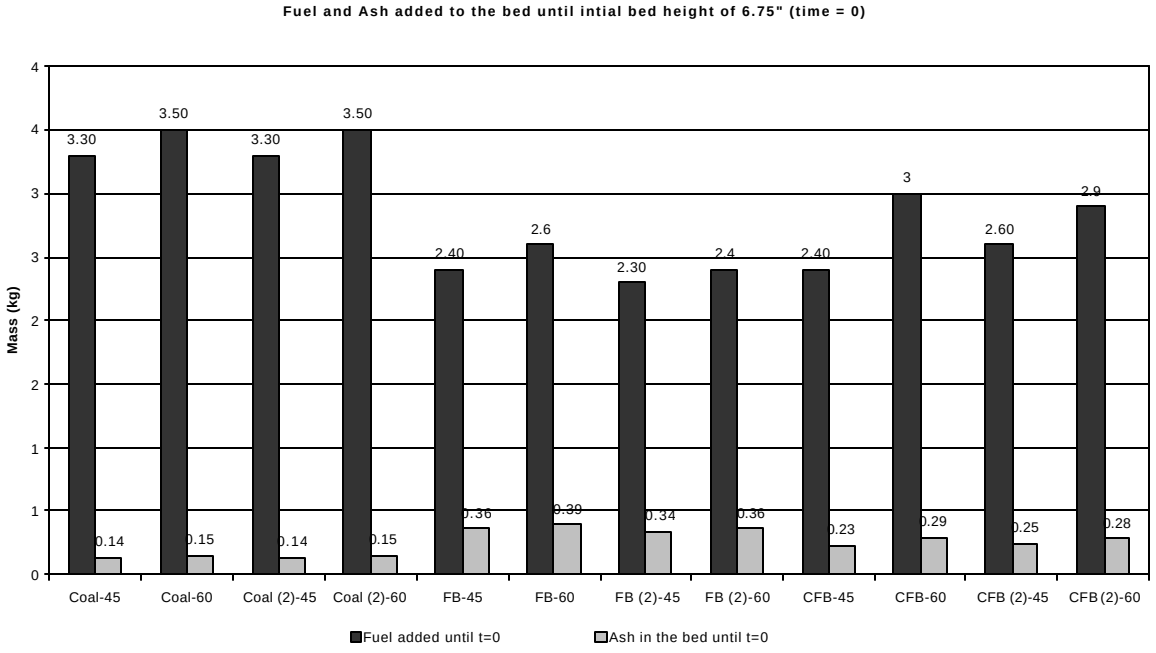

Figure A: Comparison of fuel added to attain the initial bed height of 6.75".

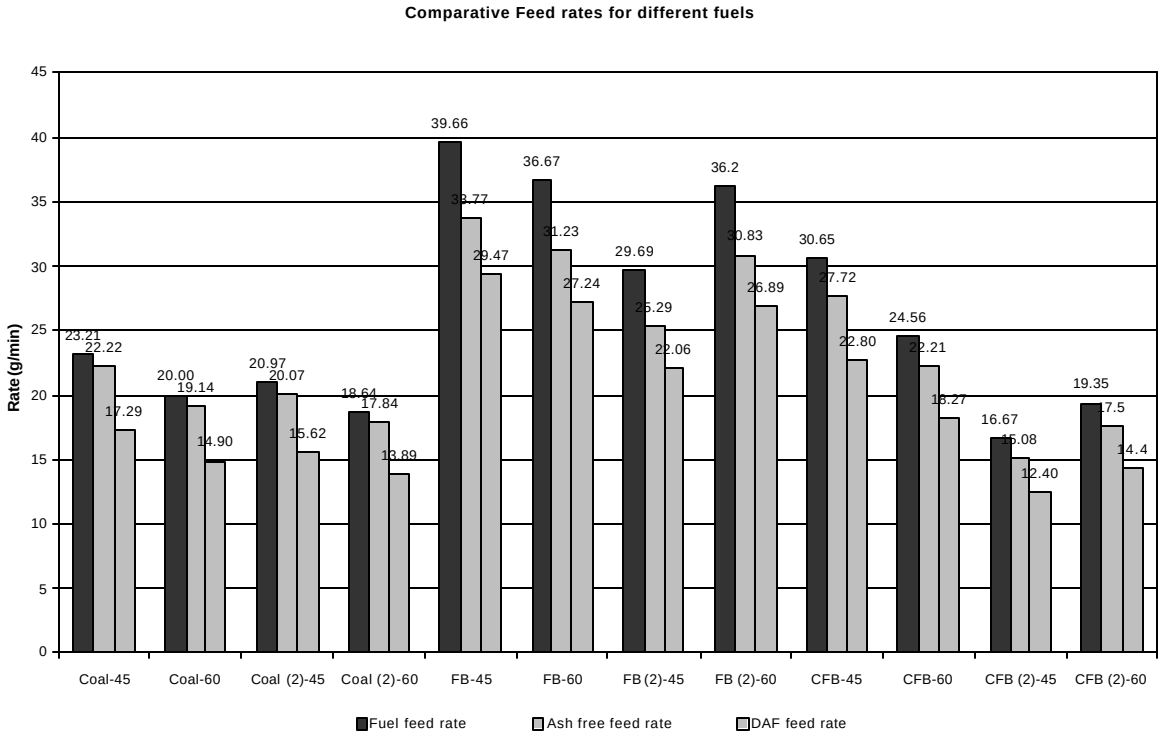

Figure B: Comparative fuel feed rates for different fuels.

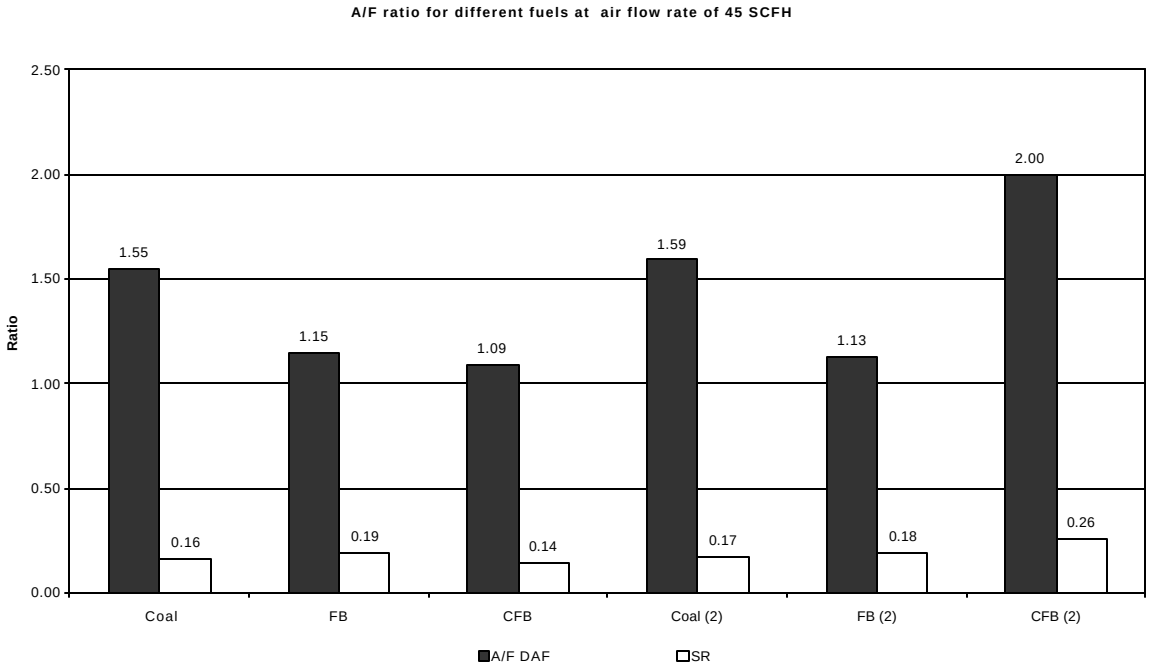

Figure C: Comparison of $A/F_{(DAF)}$ basis for different fuels at PA= 45 SCFH.

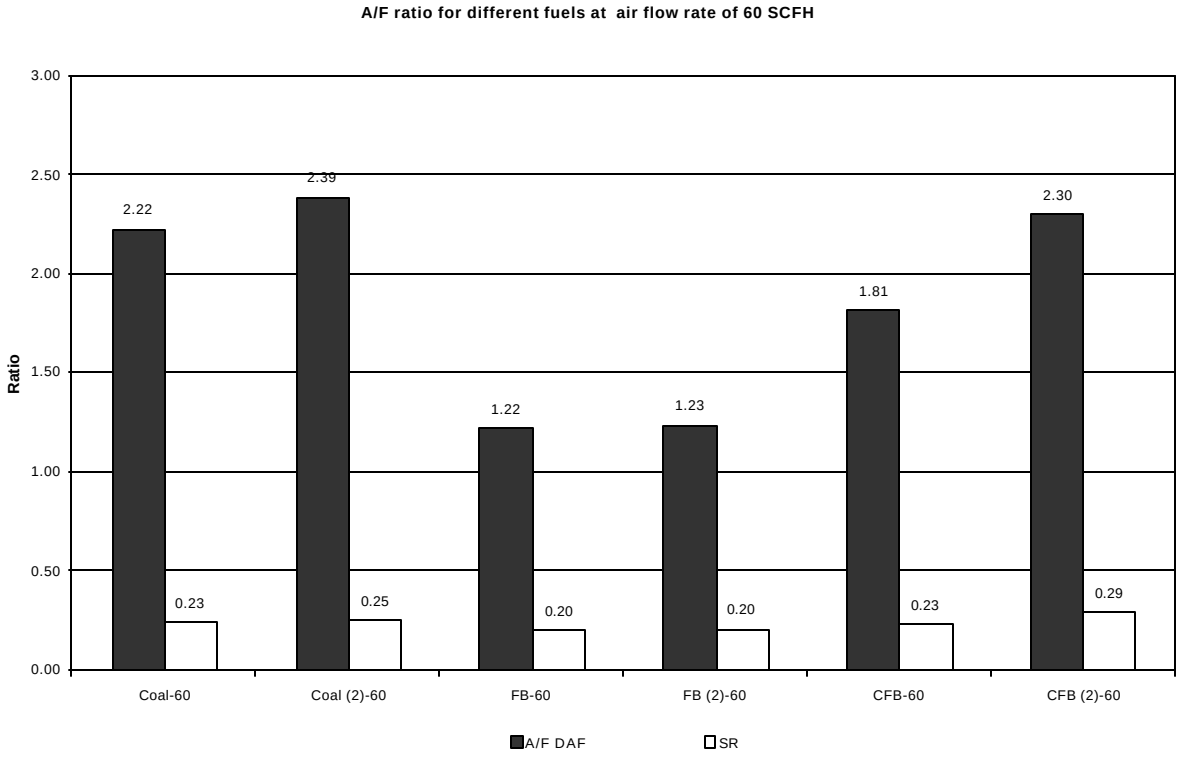

Figure D: Comparison of $A/F_{(DAF)}$ basis for different fuels at PA= 60 SCFH.

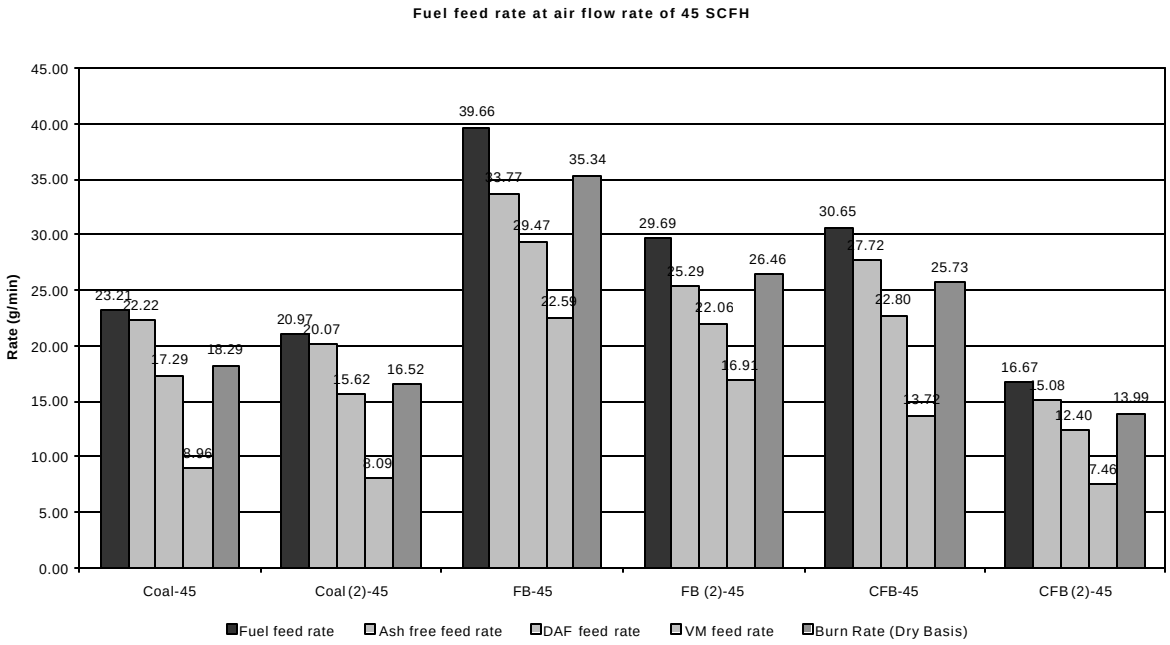

Figure E: Comparison of Feed rates for different fuels at PA= 45 SCFH.

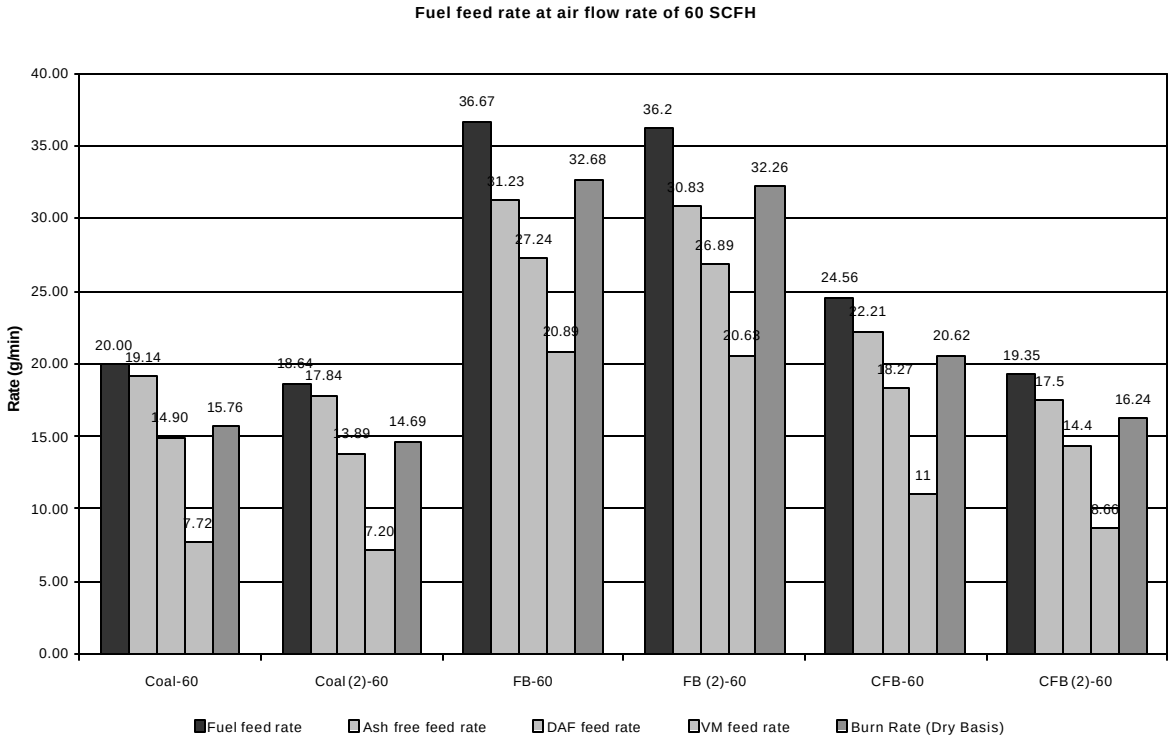

Figure F: Comparison of Feed rates for different fuels at PA= 60 SCFH.

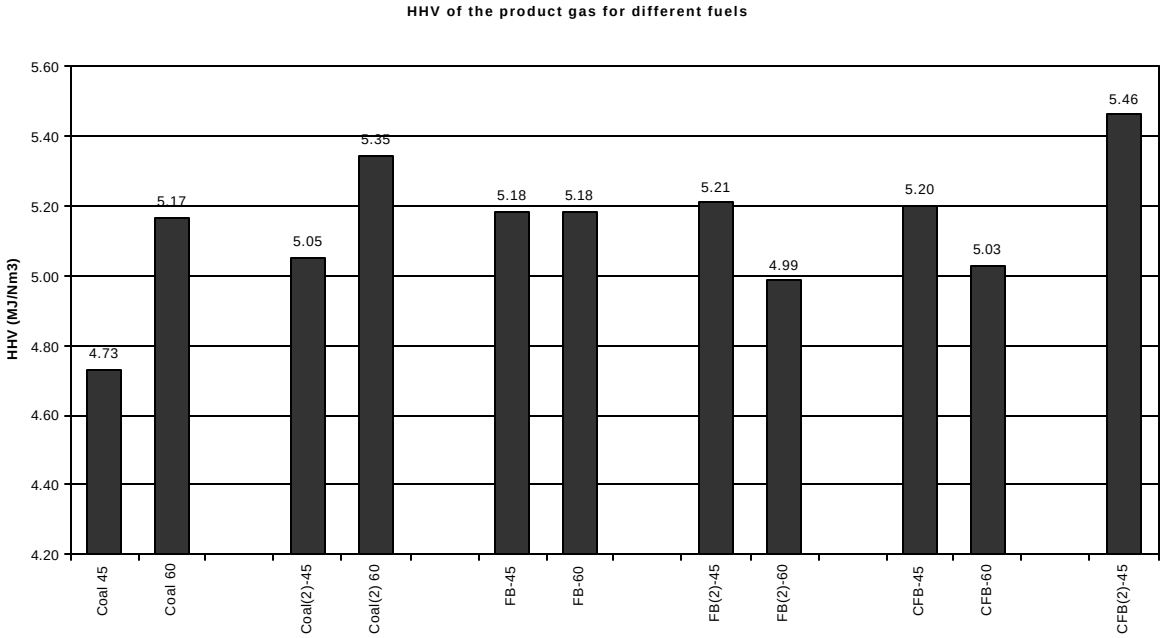

Figure G: HHV of the product gas for different fuels under different operating conditions

Appendix C: Numerical Study of Cofiring of Pulverized Coal and Litter Biomass (Task 4)

Numerical predictions were conducted for different levels of excess air (5%, 10%, 15% and 20%) and the secondary swirl number (0.7 and 1.0), and their results were compared with the existing experimental measurements. Trends of species distributions were predicted well. Effects of swirl number and excess air to combustion behavior and pollutant emissions were analyzed. Finally, numerical predictions were conducted with different moisture levels (10%, 20% and 30%) to study moisture effect to flame structure and major species emissions. The following conclusions can be drawn.

1. Two factors influences distributions and emissions of PO_2 and P_4O_{10}: temperature and oxygen. At moderately high temperature (less than 1400 K), phosphor mainly takes the form of P_4O_{10}. At high temperature around 2000 K, P_4O_{10} is negligible while PO_2 is the main phosphorous product. As oxygen concentration increases, more PO_2 is transformed into P_4O_{10}. P_4O_{10} has high concentration (200 ppm or so for 90:10 coal-LB blend) mainly in the flame core but is very low in the post-flame region. PO_2 is unimportant before flame but has high concentration in the post flame region. At the end of furnace, PO_2 level is high (e.g., around 300 ppm for 90:10 coal-LB blend) but P_4O_{10} is negligible (less than 10 ppm for 90:10 coal-LB blend).
2. Increasing moisture content in fuel blend takes more heat from gas and particle phases during vaporization thus delays pyrolysis and char combustion causing longer flame length, colder flame core, and lower burnout. As the moisture content increases, 1) in the near burner region, CO level decreases while CO_2 and H_2 levels increase; 2) in the post-flame region, CO increases and CO_2 decreases; 3) NO emission decreases with increasing the moisture content, 4) PO_2 and P_4O_{10} emissions do not change obviously. The pollutant emissions at furnace end for different levels of moisture in fuel blend are summarized in Table 4.1. Effects of blend moisture on locations of flame and near burner pollutant peaks are summarized in Table 4.2.

Table 4.1 Summary of pollutant levels at furnace end for coal-LB blend combustion with 0.7 swirl numbers, 10% excess air, and different moisture level in fuel blend

Moisture in Blend (%)	10	20	30
NO (kg/GJ)	0.209	0.200	0.189
CO (ppm)*	6033	6690	7719
P_4O_{10} (ppm)*	7.05	7.89	8.61
PO_2 (ppm)*	274.3	257.5	244.4
Burnout	0.909	0.891	0.873

* Cross-sectional averaged concentration

Table 4.2 Effects of swirl number, excess air percentage, and moisture level in fuel blend on locations of flame pollutant peaks near burner.

	Increasing swirl number	Increasing excess air percentage	Increasing moisture in fuel blend
Flame location	←	←	→
Peak CO	←	←	→
Peak CO_2	←	←	→
Peak NO	←	←	→
Peak PO_2	←	←	→
Peak P_4O_{10}	←	←	→

← Closer to burner
→ Farther away from burner

3. When biomass fraction in fuel blend is low (e.g., 10%), effects of biomass moisture to combustion behavior and species emissions are negligible.
4. Swirl number has significant effects to coal-LB blend combustion. Increasing the swirl number leads to stronger flow recirculation near burner, stronger air-fuel mixing, and shorter flame length. As swirl number increases, CO emission decreases while NO and CO_2 emissions increases due to better air-fuel mixing. There exist two opposite trends for NO production near burner: 1) higher swirl number increases air-fuel mixing causing higher NO production, and 2) higher swirl number caused shorter flame which entrains less air before flame causing less NO production. The first trend is stronger than the second one. The pollutant emissions at furnace end for different swirl numbers are summarized in Table 4.3. Effects of swirl number on locations of flame and near burner pollutant peaks are summarized in Table 4.2.

Table 4.3 Summary of pollutant levels at furnace end for coal-LB blend combustion with different swirl numbers and 10% excess air

Swirl Number	0.7	1.0
NO (kg/GJ)	0.255	0.279
CO (ppm)*	4776	4031
P_4O_{10} (ppm)*	7.95	6.11
PO_2 (ppm)*	262.7	277
Burnout	0.887	0.903

* Cross-sectional averaged concentration

5. Excess air has significant effects on flow field, flame structure, and species distributions. Increasing the excess air causes not only higher oxygen availability but also stronger recirculation flow near burner, stronger air-fuel mixing, and shorter flame length. As excess air increases, 1) temperature decreases in downstream region for fuel lean combustion; 2) burnout increases in post-flame region; 3) NO level increases in downstream region causing higher NO emission; 4) CO level decreases in furnace causing less CO emission; 3) CO_2 level may decrease slightly in downstream region, but CO_2 emission increases due to increased flow rate of flue gases; 4) P_4O_{10} level increases in downstream region increases causing more

P_4O_{10} emission; 5) PO_2 level in downstream region decreases causing less PO_2 emission. The pollutant emissions at furnace end for different excess air percentages are summarized in Table 4.4. Effects of excess air percentage on locations of flame and near burner pollutant peaks are summarized in Table 4.2.

Table 4.4 Summary of pollutant levels at furnace end for coal-LB blend combustion with 0.7 swirl numbers and different excess air percentages

Excess air (%)	5	10	15	20
NO (kg/GJ)	0.201	0.255	0.297	0.324
CO (ppm)*	5333	4776	3981	3524
P_4O_{10} (ppm)*	6.87	7.95	9.06	10.37
PO_2 (ppm)*	271.4	262.7	253.5	242.8
Burnout	0.861	0.887	0.909	0.928

* Cross-sectional averaged concentration